# One from many: Estimating a function of many parameters

Jonathan A. Gross<sup>1,2,3,\*</sup> and Carlton M. Caves<sup>1,†</sup>

<sup>1</sup>Center for Quantum Information and Control,
University of New Mexico, Albuquerque NM 87131-0001, USA

<sup>2</sup>Centre for Engineered Quantum Systems,
School of Mathematics and Physics,

The University of Queensland, St. Lucia QLD 4072, Australia

<sup>3</sup>Institut Quantique and Départment de Physique,
Université de Sherbrooke, Québec J1K 2R1, Canada

(Dated: January 27, 2023)

# Abstract

Difficult it is to formulate achievable sensitivity bounds for quantum multiparameter estimation. Consider a special case, one parameter from many: many parameters of a process are unknown; estimate a specific linear combination of these parameters without having the ability to control any of the parameters. Superficially similar to single-parameter estimation, the problem retains genuinely multiparameter aspects. Geometric reasoning demonstrates the conditions, necessary and sufficient, for saturating the fundamental and attainable quantum bound in this context.

#### I. INTRODUCTION

Well-traveled is the path of deriving quantum bounds on the sensitivity of estimating a single parameter. Fisher information <sup>1–5</sup> provides the necessary concept. Marrying Fisher information to quantum measurement theory—a marriage made in heaven!—yields the quantum Cramér-Rao bound (QCRB) on estimating a single parameter. <sup>6–11</sup> Less traveled is the deceptively similar trail of estimating a function of several parameters. Similar, yes, yet not merely a recasting of the single-parameter problem, this is a different problem with genuinely multiparameter connotations.

For those venturing onto this path, this paper formulates a roadmap for navigating the tricky terrain. Our work, challenged into existence by Eldredge et al., <sup>12</sup> explores the bound, presented there, on estimating a function of the parameters. Our goals: examine and interpret this bound, relating it to the standard bound on estimating a single parameter; formulate the quantum version in terms of a QCRB; find the necessary and sufficient conditions for saturation of the quantum bound. The key to achieving these goals comes, surprisingly, from differential geometry: respect the distinction between tangent vectors and differential forms, a distinction obscured and suppressed by a parochial preoccupation with single-parameter estimation.

A variety of previous work has considered the task we set for ourselves here. The review by Sidhu and Kok provides an overview in its Sec. VIII.B.<sup>13</sup> A typical approach to avoiding the pitfalls of single-parameter thinking is to calculate genuine multiparameter-estimation bounds and from these to extract a function-estimation bound (see work by Paris<sup>14</sup> and, more recently, by Proctor  $et~al.^{15,16}$ ). While successful, such an approach obscures the fundamental geometry of the problem through the introduction of extraneous ingredients and suffers from uncertainty in the saturability of some bounds. By identifying the relevant geometric objects, we address both issues.

Unusual, it might be thought, is the style of this paper. An explanation is in order. Kip Thorne's recent biographical memoir<sup>17</sup> of John A. Wheeler reminded us of Wheeler's passion to geometrize Einstein's general relativity and of the idiosyncratic, yet compelling writing style Wheeler used to promote that passion. Possessing a similar passion to geometrize metrology—less grand, to be sure, than Wheeler's goals, but passionate nonetheless—we adopt here Wheeler's style. As compelling we hope to be, but failing that, as idiosyncratic.<sup>18</sup>

# II. SETTING UP THE PROBLEM

Specify the problem of interest: estimate a property of a physical process through repeated interactions. Assume the physical process belongs to a family of quantum channels  $\mathcal{E}_{\tilde{\theta}}$  parametrized by  $\tilde{\theta} = (\theta^1, \dots, \theta^N)$  and the property is a function  $q(\tilde{\theta})$  of these parameters. Consider interacting with the process by preparing a quantum system in a chosen state, subjecting the system to the evolution the process dictates, and finally measuring the evolved system. Perform many such interactions, and estimate the property of interest based on the data obtained. Pose now the natural question: what is the best precision with which the property can be estimated?

A luxury that guarantees proximity to the truth are the many interactions with the process. Indulge therefore in an initial estimate for the process encoded in a parameter point  $\tilde{\theta}_0$  near to the true parameter point. Lock the interactions to this fiducial operating point. Precision then describe by the extent to which small deviations of the truth from  $\tilde{\theta}_0$ 

can be detected.

Reify the setup through two examples. To estimate a phase shift  $\varphi$  in the presence of an unknown loss rate  $\gamma$ , coördinates  $\tilde{\theta} = (\varphi, \gamma)$  parametrize the process, and the function is simply  $q(\varphi, \gamma) = \varphi$ . To estimate the average fidelity of a process with respect to a target unitary  $\mathcal{U}$ , coördinates  $\tilde{\theta}$  parametrize the family of all quantum channels, and  $q(\tilde{\theta}) = \int d\psi \langle \psi | (\mathcal{U}^{-1} \circ \mathcal{E}_{\tilde{\theta}}) (|\psi\rangle \langle \psi |) |\psi\rangle$ .

Unitary processes occupy much of our attention in this exposition, so additional comments peculiar to this case are in order. Transform the family of interest  $\mathcal{V}_{\tilde{\theta}}$  to the equivalent family  $\mathcal{U}_{\tilde{\theta}} = \mathcal{V}_{\tilde{\theta}} \circ \mathcal{V}_{\tilde{\theta}_0}^{-1}$ ; the fiducial parameter point  $\tilde{\theta}_0$  then corresponds to the identity process,  $\mathcal{U}_{\tilde{\theta}_0} = \mathcal{I}$ . Convenient it is to parametrize this unitary by its Hamiltonian  $H(\tilde{\theta})$ ,

$$\mathcal{U}_{\tilde{\theta}}(\rho) = e^{-iH(\tilde{\theta})} \rho e^{iH(\tilde{\theta})} \,. \tag{2.1}$$

The motivating work by Eldredge *et al.*<sup>12</sup> considered a Hamiltonian for a set of spins and a property q, both assumed to be linear in the chosen parametrization  $\tilde{\theta}$ ,

$$H(\tilde{\theta}) = \frac{1}{2} \sum_{j} \theta^{j} \sigma_{j}^{z} = \frac{1}{2} \theta^{j} \sigma_{j}^{z}, \qquad (2.2)$$

$$q(\tilde{\theta}) = \sum_{j} \alpha_{j} \theta^{j} = \alpha_{j} \theta^{j}. \tag{2.3}$$

The last forms introduce the Einstein summation convention: sum over index labels that occur simultaneously in a lower and an upper position within an expression. Though arbitrary Hamiltonians and properties are not linear functions of a parametrization, write linear approximations to them in the neighborhood of the fiducial point  $\tilde{\theta}_0$ :

$$H(\tilde{\theta}_0 + d\tilde{\theta}) = H(\tilde{\theta}_0) + d\theta^j \, \partial_j H|_{\tilde{\theta}_0} = d\theta^j X_j \,, \tag{2.4}$$

$$q(\tilde{\theta}_0 + d\tilde{\theta}) = q(\tilde{\theta}_0) + \partial_j q|_{\tilde{\theta}_0} d\theta^j = q(\tilde{\theta}_0) + q_j d\theta^j.$$
(2.5)

Here and throughout, employ the shorthand  $\partial_j = \partial/\partial\theta^j$  to harmonize with the summation convention. Also eliminated is  $H(\tilde{\theta}_0)$ , set to zero since  $\mathcal{U}_{\tilde{\theta}_0} = \mathcal{I}$ . Further, reparametrize to choose  $\tilde{\theta}_0 = 0$  and to set  $q(\tilde{\theta}_0) = 0$ .

Justified indeed are these linear approximations when bounding optimal estimation, as the limit of many interactions is our concern and the uncertainty in  $\tilde{\theta}$  in this limit is correspondingly small. Press this point home: estimation in the limit of many experiments is properly studied in the tangent space to the parameter manifold at a fiducial point. This perspective we develop in greater detail in the following section.

# III. CLASSICAL ESTIMATION: EXERCISING YOUR DIFFERENTIAL GEOMETRY

Tangent vectors, differential forms, and metrics: these basic elements from differential geometry provide the mathematical language for the estimation problem. Generally forgotten in the parameter-estimation literature are differential forms, mainly due to a focus on single-parameter problems. Worthy of our meditation and attention day and night, renew now acquaintance with these geometric objects.

#### A. Classical Fisher information

Understand first the classical problem of estimating the parameters specifying a given probability distribution within a parametrized family of distributions  $p(x|\tilde{\theta})$ , reserving for subsequent sections the issue of choosing initial system state and final system measurement that transform our parametrized family of quantum channels into such a family of distributions.

The classical procedure is straightforward: sample data x from the conditional probability  $p(x|\tilde{\theta})$  and use hatted function  $\hat{\theta}^{j}(x)$  to estimate the parameter  $\theta^{j}$  from the data. The covariance matrix of the estimators,

$$C^{jk} = \operatorname{Cov}(\hat{\theta}^j, \hat{\theta}^k) = \int dx \, p(x|\tilde{\theta}) \left[ \hat{\theta}^j(x) - \langle \hat{\theta}^j \rangle_{\tilde{\theta}} \right] \left[ \hat{\theta}^k(x) - \langle \hat{\theta}^k \rangle_{\tilde{\theta}} \right], \tag{3.1}$$

captures a notion of the accuracy of the estimates. In this definition,

$$\langle \hat{\theta}^j \rangle_{\tilde{\theta}} = \int dx \, p(x|\tilde{\theta}) \hat{\theta}^j(x)$$
 (3.2)

is the mean value of the estimator  $\hat{\theta}^j(x)$ , and the parameters  $\tilde{\theta} = (\theta^1, \dots, \theta^N)$  should be regarded as true values.

The deviations  $\hat{\theta}^j(x) - \langle \hat{\theta}^j \rangle_{\tilde{\theta}}$  express how far the estimates depart from the mean value. Better it might be thought to use as deviations the difference between the estimate and the true value,  $\hat{\theta}^j(x) - \theta^j$ ; this usage replaces the covariance matrix with the error-correlation matrix. An unbiased estimator has mean values equal to true values, *i.e.*,  $\langle \hat{\theta}^j \rangle_{\tilde{\theta}} = \theta^j$ . Appendix A demonstrates how to extract an unbiased estimator from a biased estimator. Specialize now and henceforth to unbiased estimators, thus making the error-correlation matrix identical to the covariance matrix.

The Fisher-information matrix,

$$F_{jk} = \int dx \, p(x|\tilde{\theta}) \partial_j \ln p(x|\tilde{\theta}) \, \partial_k \ln p(x|\tilde{\theta}) = \int dx \, \frac{1}{p(x|\tilde{\theta})} \partial_j p(x|\tilde{\theta}) \, \partial_k p(x|\tilde{\theta}) \,, \tag{3.3}$$

is the foundation on which rests classical multiparameter-estimation theory. For the small deviations from the fiducial operating point contemplated in this paper, the integrands in the expressions for the covariance matrix and the Fisher matrix should be evaluated at the fiducial point, *i.e.*,  $\tilde{\theta} = \tilde{\theta}_0$ .

Foundation because the covariance matrix satisfies the matrix inequality

$$C \ge F^{-1},\tag{3.4}$$

called the multiparameter (classical) Cramér-Rao bound (CCRB). Achieving the CCRB generally requires working in the asymptotic limit of many trials and requires using the right estimators—maximum-likelihood estimation works. Assume here and hereafter an appropriate estimator and sufficient trials to achieve the CCRB.

To understand the message of the CCRB, learn now to inhabit the linearized neighborhood of the fiducial point  $\tilde{\theta}_0$ . Of primary importance is appreciating an important distinction: measuring changes in the property q along a particular path corresponding to varying

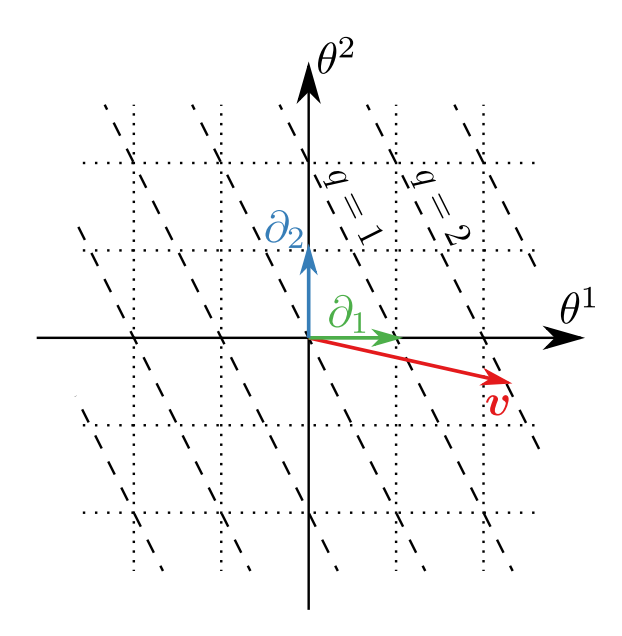


FIG. 1. Level surfaces of linear combination  $q = q_j \theta^j$ , here taken to be  $q = \theta^1 + \frac{1}{2}\theta^2$ . This example for parameter q is used throughout in figures for two coördinate dimensions (three-dimensional Fig. 12 uses  $q = \theta^1 + \frac{2}{3}\theta^2 + \frac{1}{3}\theta^3$ ). The vector  $\mathbf{v}$ , here taken to be  $\mathbf{v} = \frac{9}{4}\partial_1 - \frac{1}{2}\partial_2$ , extends through two units of q, this expressed by  $dq(\mathbf{v}) = \mathbf{v}(q) = 2$ . The level surfaces of the parameters  $\theta^1$  and  $\theta^2$  define a square grid. The directional-derivative basis vector  $\partial_{1,2} = \partial/\partial\theta^{1,2}$  lies in a level surface of  $\theta^{2,1}$  and extends one unit in  $\theta^{1,2}$ . Neatly summarizing this description is the grid equation  $d\theta^j(\partial_k) = \partial_k \theta^j = \delta^j_k$ . No notion of length and orthogonality yet—the square grid for  $\theta^1$  and  $\theta^2$  is used only for convenience.

a linear combination of the parameters  $\theta^j$  requires bringing together two distinct geometric objects, one that characterizes how q changes as the parameters  $\theta^j$  wander around the neighborhood and another that identifies the particular path.

Call the linearized neighborhood of the fiducial point  $\theta_0$  by its formal name, the tangent space. Represent a small displacement  $\boldsymbol{v}$  on the tangent space graphically by an arrow, as done in Fig. 1, and algebraically by a directional (partial) derivative,

$$\mathbf{v} = v^j \partial_j \,. \tag{3.5}$$

The vector  $\boldsymbol{v}$  is a linear combination of the directional derivatives  $\partial_j$  associated with the coördinates  $\theta^j$ .

Represent the property q graphically on the tangent space by its level surfaces, as is done in Fig. 1, and algebraically by a differential form,

$$dq = q_j d\theta^j. (3.6)$$

Notice that dq is a linear combination of the differential forms  $d\theta^{j}$  associated with the level surfaces of the coördinates  $\theta^{j}$ ; together, the level surfaces of all the coördinates define the familiar coördinate grid (see Fig. 1).

The differential form dq characterizes how q changes in the linear neighborhood of the fiducial point and is poised to measure the change in the value of q effected by a vector v

in the tangent space:

$$dq(\mathbf{v}) = \mathbf{v}(q) = v^j \partial_j q = q_j v^j \tag{3.7}$$

is the difference between the value of q at the tip of v and the value of q at the tail of v (located at the origin).

The parametrization  $\tilde{\theta}$  defines a basis of forms and a basis of vectors dual to one another in the sense that  $\partial_j$  lies within the zero surface of all  $d\theta^{k\neq j}$  and extends to the unit surface of  $d\theta^j$ . Summarizing the pictorial properties of the coördinate grid is a compact set of equations:

$$d\theta^{j}(\partial_{k}) = \frac{\partial \theta^{j}}{\partial \theta^{k}} = \delta^{j}_{k}. \tag{3.8}$$

This formalizes the important distinction: differential forms characterize how a quantity like q varies in the linear neighborhood of the fiducial point; vectors specify movement in the tangent space.

Constructed by taking directional derivatives, the Fisher-information matrix (3.3) has a natural expression as a (covariant) 2-tensor,

$$\mathbf{F}_{\downarrow} = F_{jk} \, d\theta^j \otimes d\theta^k \,, \tag{3.9}$$

on the tangent space. Indeed, manifestly symmetric and positive is the Fisher-information matrix, so it is a Riemannian metric on the tangent space, providing a prescription for taking inner products between vectors,

$$\langle \boldsymbol{u}, \boldsymbol{v} \rangle_F = F_{jk} u^j v^k = \boldsymbol{F}_{\downarrow}(\boldsymbol{u}, \boldsymbol{v}).$$
 (3.10)

The matrix elements  $F_{jk}$  are the inner products  $\mathbf{F}_{\downarrow}(\partial_j, \partial_k)$ . Positive the Fisher-information matrix might be, but it can have zero eigenvalues. Care is required in dealing with degenerate Fisher-information matrices, as is evident from the CCRB (3.4). Proceed now with caution, assuming the Fisher-information matrix is strictly positive; return to the question of degenerate Fisher matrices at the end of Sec. III D.

Each vector  $\boldsymbol{v}$  defines a single-parameter estimation problem by locally restricting the family of distributions to parameter variations that give displacements along  $\boldsymbol{v}$ . The Fisher information for this single-parameter problem is the scalar

$$F_{vv} = \int dx \frac{1}{p(x|\tilde{\theta})} \boldsymbol{v} (p(x|\tilde{\theta})) \boldsymbol{v} (p(x|\tilde{\theta}))$$

$$= \int dx \frac{1}{p(x|\tilde{\theta})} v^{j} \partial_{j} p(x|\tilde{\theta}) v^{k} \partial_{k} p(x|\tilde{\theta}) = \boldsymbol{F}_{\downarrow}(\boldsymbol{v}, \boldsymbol{v}).$$
(3.11)

Pause to savor that the Fisher-information tensor holds within itself the CCRB for all single-parameter problems.

More explicit we can be about the single-parameter estimation problem specified by  $\mathbf{v}$ : vary and estimate a parameter  $\phi = \phi^1$  satisfying  $d\phi(\mathbf{v}) = 1$ , while holding fixed N-1 other parameters  $\phi^j$ , j = 2, ..., N, satisfying  $d\phi^j(\mathbf{v}) = 0$ . In words, considering  $(\phi^1, ..., \phi^N)$  as a local coördinate system,  $\mathbf{v}$  extends one unit in  $\phi$  and points in the direction obtained by varying  $\phi$  while holding the other coördinates fixed (see Fig. 2); implied is that  $\mathbf{v} = \partial/\partial\phi$ .

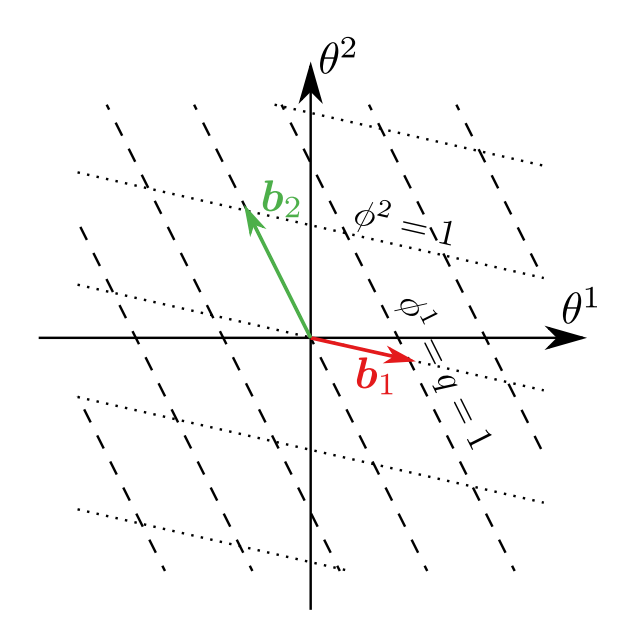


FIG. 2. Natural coördinate grid relative to the level surfaces of q, natural because one of the parameters, call it  $\phi^1$ , is equal to q. Read the  $(\phi^1, \phi^2)$  coördinates of a parameter point by identifying the level surfaces of  $\phi^1$  and  $\phi^2$  in which the point lies. The basis vectors (directional derivatives) are  $\mathbf{b}_j = \partial/\partial\phi^j = b^k{}_j\partial_k$ . That  $\phi^1 = q$  means that  $\mathbf{b}_1$  advances one unit in q [ $dq(\mathbf{b}_1) = 1$ ] and that  $\mathbf{b}_2$  lies in the q = 0 level surface means that  $dq(\mathbf{b}_2) = 0$ . Enough to define a single-parameter estimation problem these conditions are not, because  $\mathbf{b}_1$ , along which  $\phi^1$  advances, can point to any location on the plane q = 1, its direction determined by the other parameters; specifically, the direction of  $\mathbf{b}_1$  is determined by varying  $\phi^1$  while holding  $\phi^2$  constant  $[d\phi^2(\mathbf{b}_1) = 0]$ .

The scalar Fisher information (3.11) bounds the single-parameter estimator variance (keep in mind the assumption of unbiased estimators,  $\langle \hat{\phi} \rangle_{\tilde{\theta}} = \phi$ ),

$$\Delta \hat{\phi}^2 = \int dx \, p(x|\tilde{\theta}) \left[ \hat{\phi}(x) - \phi \right]^2 \ge \frac{1}{F_{vv}} = \frac{1}{F_{\perp}(\boldsymbol{v}, \boldsymbol{v})}. \tag{3.12}$$

Find a fuller understanding of coördinate systems matched to single-parameter estimation in Sec. III C.

The inverse of the Fisher-information matrix is the optimal covariance matrix, which measures deviations of parameter estimates from the true parameter value. Since measuring deviations is the job of differential forms, learn with satisfaction that the natural formulation of the inverse Fisher-information matrix is as a (contravariant) 2-tensor,

$$\mathbf{F}^{\uparrow} = (F^{-1})^{jk} \, \partial_j \otimes \partial_k = F^{jk} \, \partial_j \otimes \partial_k, \tag{3.13}$$

which provides a prescription for calculating (optimal) covariances of parameters specified by forms,

$$Cov(\hat{\theta}^j, \hat{\theta}^k) = F^{jk} = \mathbf{F}^{\uparrow}(d\theta^j, d\theta^k). \tag{3.14}$$

# B. Scalar estimation

No control of any of the parameters, no prior constraints on how any parameter varies, no ability to hold any combination of the parameters fixed—these mean that an estimate of q must be extracted from estimating all the parameters. Uncertainties in the estimates of all the parameters feed into the uncertainty in the estimate of q.

From the parameter estimators  $\hat{\theta}^{j}(x)$  comes an estimator  $\hat{q}(x)$ , the same linear combination as q is a linear combination of the parameters  $\theta^{j}$ :

$$\hat{q}(x) = q_j \hat{\theta}^j(x) \,. \tag{3.15}$$

The estimator variance

$$\Delta \hat{q}^2 = \int dx \, p(x|\tilde{\theta}) \left[ \hat{q}(x) - q \right]^2 = q_j q_k \int dx \, p(x|\tilde{\theta}) \left[ \hat{\theta}^j(x) - \theta^j \right] \left[ \hat{\theta}^k(x) - \theta^k \right]$$
(3.16)

—recall the assumption of unbiased estimators, for which  $\langle \hat{q} \rangle_{\tilde{\theta}} = q$ —is the action of the covariance matrix (3.1), written as a contravariant 2-tensor  $C^{\uparrow}$ , on the form dq:

$$\Delta \hat{q}^2 = C^{jk} q_j q_k = \mathbf{C}^{\uparrow} (dq, dq) \,. \tag{3.17}$$

The matrix CCRB (3.4) provides the one-from-many, no-control CCRB,

$$\Delta \hat{q}^2 = \mathbf{C}^{\uparrow}(dq, dq) \ge \mathbf{F}^{\uparrow}(dq, dq).$$
 (3.18)

Implicated here is the invariant constructed from the contravariant form of the Fisher metric,  $\mathbf{F}^{\uparrow}$ , and the 1-form dq:

$$\mathbf{F}^{\uparrow}(dq, dq) = F^{jk}q_i q_k = q_i q^j. \tag{3.19}$$

Raise the index on dq using  $\mathbf{F}^{\uparrow}$ , and find the vector  $\mathbf{q}_F = q^j \partial_j$  introduced in the last form,

$$q^j = F^{jk}q_k. (3.20)$$

Orthogonal to the level surfaces of q, according to the Fisher metric, is  $q_F$ :

$$\langle \boldsymbol{q}_F, \boldsymbol{v} \rangle_F = \boldsymbol{F}_{\downarrow}(\boldsymbol{q}_F, \boldsymbol{v}) = F_{ik}q^jv^k = q_kv^k = dq(\boldsymbol{v}) = 0,$$
 (3.21)

for any v that lies in the level surfaces of q. Express the invariant (3.19) in all its forms,

$$F^{jk}q_{j}q_{k} = \mathbf{F}^{\uparrow}(dq, dq)$$

$$= F_{jk}q^{j}q^{k} = \mathbf{F}_{\downarrow}(\mathbf{q}_{F}, \mathbf{q}_{F}) = \langle \mathbf{q}_{F}, \mathbf{q}_{F} \rangle_{F}$$

$$= q_{j}q^{j} = dq(\mathbf{q}_{F}).$$
(3.22)

Pause to appreciate that no-control estimation is controlled by this invariant.

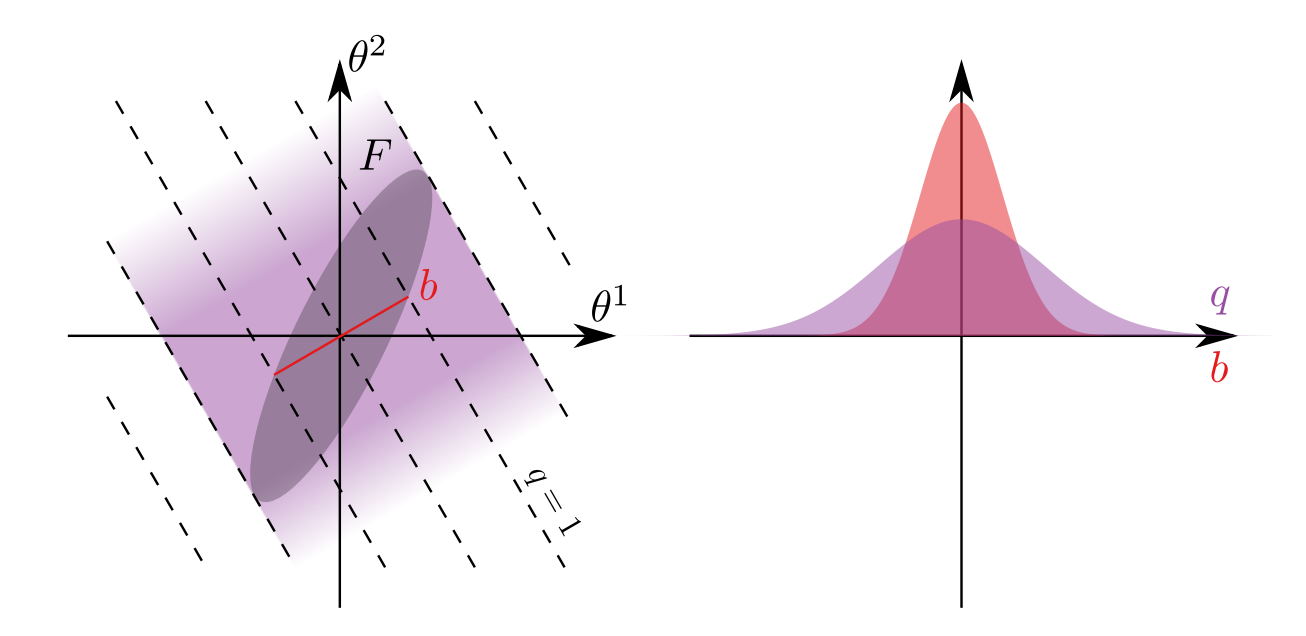


FIG. 3. The Fisher information for a multiparameter family of probability distributions gives the smallest covariance of estimates about the true parameter values. The Fisher information for a single parameter in this setting gives the smallest variance of estimates of that parameter about its true value, conditioned on knowledge of the true values of the other parameters (here illustrated by the parameter b). The smallest variance of estimates of the value of a function of the parameters about its valuation at the true parameter values is given by the variance of the multiparameter-estimate distribution marginalized over parameters that don't change the function value (here illustrated by the level surfaces of the function q). The probability densities at right illustrate how the conditional distribution of a parameter associated with the function values is generally narrower than the limit given by the marginal of the Fisher information.

# C. Scalar estimation is not single-parameter estimation

Address now the pitfalls in neglecting the distinction between forms and vectors. Reparametrize the tangent space with new coördinates  $\tilde{\phi} = (\phi^1, \dots, \phi^N)$ . Match these coördinates to the job of estimating q by calling out one of the new coördinates, make it the first, to be q itself, i.e.,  $\phi^1 = q$ , with associated differential form

$$d\phi^1 = dq = q_j d\theta^j \,. \tag{3.23}$$

Emerging from these new coördinates are new directional derivatives,

$$\frac{\partial}{\partial \phi^j} = \mathbf{b}_j = b^k{}_j \partial_k \,, \tag{3.24}$$

their vectorial character highlighted by the special designation  $\boldsymbol{b}_j$ . Choose now to omit the subscript on the special coördinate  $\phi^1$  and its associated directional derivative  $\boldsymbol{b}_1$ , writing  $\phi^1 = \phi$  and  $\boldsymbol{b}_1 = \boldsymbol{b}$ . These new coördinates and their basis vectors define a new coördinate grid, characterized by the equations

$$d\phi^{j}(\boldsymbol{b}_{k}) = \boldsymbol{b}_{k}(\phi^{j}) = \delta^{j}_{k}. \tag{3.25}$$

One such new coördinate grid is illustrated in Fig. 2.

Suggested by this parametrization is a single-parameter estimation problem closely tied to the problem of estimating q:  $\boldsymbol{b}$  specifies a line through the fiducial origin in the tangent space that specifies a single-parameter manifold of distributions, and  $dq(\boldsymbol{b}) = 1$  means that the parameter  $\phi$  changes by one unit from tail to tip of  $\boldsymbol{b}$ . Alluring though this identification is, at our disposal are the tools to silence the siren's call.

Observe the difference between optimal variances of single-parameter estimation of  $\phi$  and estimation of q within a multiparameter manifold:

$$\Delta \hat{\phi}^2 \ge \frac{1}{\mathbf{F}_{\perp}(\mathbf{b}, \mathbf{b})} = (F_{jk}b^jb^k)^{-1} \tag{3.26}$$

$$\Delta \hat{q}^2 \ge \mathbf{F}^{\uparrow}(dq, dq) = (F^{-1})^{jk} q_i q_k. \tag{3.27}$$

Figure 3 illustrates the distinction between these two quantities, depicting the covariance of the full estimator as a shaded ellipse containing the tips of all vectors  $\mathbf{v}$  that represent parameter changes within a standard deviation of the origin, i.e.,  $\mathbf{F}_{\downarrow}(\mathbf{v}, \mathbf{v}) \leq 1$ . Variation in  $\hat{q}$  is clearly variation in the full estimator distribution marginalized over deviations that leave q unchanged, while variation in  $\hat{\phi}^1$  is variation in the full estimator conditioned on the other parameters being held fixed to their fiducial values.

Most importantly, variation in  $\hat{\phi}^1$  depends on an arbitrary choice of parametrization. Given only the choice  $\phi^1 = q$ ,  $\boldsymbol{b}_1$  can place its tip at any point on the plane q = 1; its direction, required to specify a single-parameter problem, is determined by the coördinates that accompany  $\phi^1$ . Specifically,  $\boldsymbol{b}_1$  points in the direction determined by holding the other coördinates fixed:

$$d\phi^{j}(\boldsymbol{b}_{1}) = 0, \quad j = 2, \dots, N.$$
 (3.28)

Free we are to modify  $b_1$  by adding to it any vector lying in the null surface of q—that is, any linear combination of  $b_2, \ldots, b_N$ . Such a modification of  $b_1$  drags along the coördinates  $\phi^2, \ldots, \phi^N$ , ensuring they still satisfy Eq. (3.28). Different choices for  $b_1$  pick out different single-parameter submanifolds. The variance of  $\hat{\phi}^1$  measures estimator precision for these irrelevant single-parameter problems. Variation in  $\hat{q}$  rises above petty differences in parametrizations and measures estimator precision for the no-control problem at hand.

An alternative perspective is that dq and  $\mathbf{F}^{\uparrow}$  together privilege a particular single-parameter problem whose sensitivity bound coincides with the bound for the scalar estimation problem. The vector  $\mathbf{q}_F$  defined in Eq. (3.20), orthogonal to surfaces of constant q according to the Fisher metric, is not suitably normalized to define a single-parameter estimation problem, because  $dq(\mathbf{q}_F) = q_j q^j = \langle \mathbf{q}_F, \mathbf{q}_F \rangle_F$ . Suitable it becomes by scaling it to place the tip on the unit surface of q:

$$\boldsymbol{b}_F = \frac{\boldsymbol{q}_F}{\langle \boldsymbol{q}_F, \boldsymbol{q}_F \rangle_F} \,. \tag{3.29}$$

The vector  $\boldsymbol{b}_F$  has squared Fisher length

$$F_{\downarrow}(\boldsymbol{b}_F, \boldsymbol{b}_F) = \langle \boldsymbol{b}_F, \boldsymbol{b}_F \rangle_F = \frac{1}{\langle \boldsymbol{q}_F, \boldsymbol{q}_F \rangle_F} = \frac{1}{\boldsymbol{F}^{\uparrow}(dq, dq)},$$
 (3.30)

leading to a no-control CCRB,

$$\Delta \hat{q}^2 \ge \mathbf{F}^{\uparrow}(dq, dq) = \frac{1}{\mathbf{F}_{\downarrow}(\mathbf{b}_F, \mathbf{b}_F)},$$
(3.31)

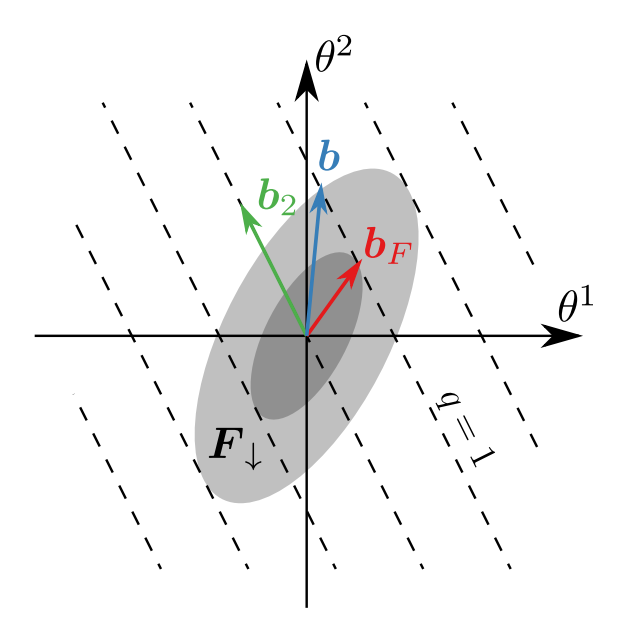


FIG. 4. Vectors of the same length according to the Fisher metric  $\mathbf{F}_{\downarrow}$  have their tips on a covariance ellipse centered at the origin. A single-parameter problem is specified by a vector  $\mathbf{b}$  that extends one unit in q; the Fisher information  $F_{bb}$  for this problem is the length of  $\mathbf{b}$  as measured by the Fisher metric. The shortest vector,  $\mathbf{b}_F$ , thus having the least Fisher information, is orthogonal to the level surfaces of q according to the Fisher metric; this smallest Fisher information governs estimation of q when one has no control over any of the parameters  $\theta^j$ . Other vectors that extend one unit in q, exemplified by  $\mathbf{b}$ , have more Fisher information, as they can be made shorter by sliding the tip along the unit surface of q toward  $\mathbf{b}_F$ . Indeed, a way of characterizing orthogonality to the level surfaces of q is that the tip of  $\mathbf{b}_F$  is at the point where the Fisher ellipse is tangent to the surface q = 1, so that any sliding of the tip of  $\mathbf{b}_F$  increases the length.

which coincides with the CCRB for single-parameter estimation defined by  $b_F$ .

Figure 4 depicts the geometry:  $b_F$ , as the vector orthogonal to level surfaces of q according to the classical Fisher metric, is the shortest vector that extends one unit in q and so has the least Fisher information of all such vectors. Consider any vector b satisfying

$$1 = dq(\mathbf{b}) = q_j b^j = F_{jk} q^j b^k = \langle \mathbf{q}_F, \mathbf{b} \rangle_F.$$
(3.32)

Cauchy-Schwarz commands, 12

$$1 = \langle \boldsymbol{q}_F, \boldsymbol{b} \rangle_F^2 \le \langle \boldsymbol{q}_F, \boldsymbol{q}_F \rangle_F \langle \boldsymbol{b}, \boldsymbol{b} \rangle_F = \frac{\langle \boldsymbol{b}, \boldsymbol{b} \rangle_F}{\boldsymbol{F}_{\downarrow}(\boldsymbol{b}_F, \boldsymbol{b}_F)}, \qquad (3.33)$$

so the Fisher information for  $b \neq b_F$  exceeds that for  $b_F$ ,

$$F_{bb} = \langle \boldsymbol{b}, \boldsymbol{b} \rangle_F \ge \boldsymbol{F}_{\downarrow}(\boldsymbol{b}_F, \boldsymbol{b}_F).$$
 (3.34)

Revealed is that the no-control bound is the most pessimistic single-parameter bound:

$$\Delta \hat{q}^2 \ge \mathbf{F}^{\uparrow}(dq, dq) = \frac{1}{\mathbf{F}_{\downarrow}(\mathbf{b}_F, \mathbf{b}_F)} \ge \frac{1}{F_{bb}}.$$
 (3.35)

# D. Interpretation

Apparently identical, yet subtly different, the variances  $\Delta \hat{\phi}^2$  of Eq. (3.26) and  $\Delta \hat{q}^2$  of Eq. (3.27) teach a lesson: in the integrals (3.12) and (3.16) for the variances, the parameters are evaluated at the fiducial point, taken here to be zero parameter values; the difference lies in that  $\Delta \hat{q}^2$  is honest about its uncertainty in all parameters, whereas  $\Delta \hat{\phi}^2$  presumes to know the true values of  $\phi^2, \ldots, \phi^N$ . Assuming  $\hat{\phi}$  has the blind luck to correctly guess  $\phi^2, \ldots, \phi^N$ , it will outperform  $\hat{q}$ . In the presence of real uncertainty, though,  $\hat{\phi}$  trips on the tangled web it wove and underperforms  $\hat{q}$ .

More enlightening still is it to understand, as is depicted in Fig. 4, that the Fisher ellipse  $\mathbf{F}_{\downarrow}(\mathbf{v},\mathbf{v}) = \mathbf{F}_{\downarrow}(\mathbf{b}_F,\mathbf{b}_F)$  is tangent to the unit level surface of q. Implied is that errors in estimates of parameters that don't change q are uncorrelated with errors in  $\mathbf{b}_F$ ; there is no danger in using an estimator that assumes incorrect values for such parameters. This insensitivity to errors in the other parameters is the reason the single-parameter problem specified by  $\mathbf{b}_F$  is the same as the no-control estimation problem for q: a single-parameter problem assumes the other parameters are fixed at their fiducial values, but for the special single-parameter problem specified by  $\mathbf{b}_F$ , this assumption is unnecessary, and the other parameters can be left uncontrolled.

Insensitivity to errors in these other parameters suggests considering Fisher matrices that are degenerate and thus not metrics at all. Of particular interest is a rank-one Fisher matrix,

$$\mathbf{F}_{\perp} = A^2 \, dq \otimes dq \,, \tag{3.36}$$

where A is a constant. The components of the Fisher matrix are

$$F_{jk} = \mathbf{F}_{\downarrow}(\partial_j, \partial_k) = A^2 \, dq(\partial_j) \, dq(\partial_k) = A^2 q_j q_k \,. \tag{3.37}$$

Constructed from dq alone, the Fisher matrix (3.36) enjoys the exalted status of the invariant  $\mathbf{F}^{\uparrow}(dq, dq) = 1/\mathbf{F}_{\downarrow}(\mathbf{b}_F, \mathbf{b}_F)$ . Any vector  $\mathbf{v}$  has Fisher information

$$\mathbf{F}_{\downarrow}(\mathbf{v}, \mathbf{v}) = F_{vv} = A^2 (q_i v^j)^2 = A^2 [dq(\mathbf{v})]^2,$$
 (3.38)

meaning that any sampling procedure giving rise to such a Fisher matrix is sensitive only to the parameter q and not to any of the other coördinates. Indeed, any vector  $\mathbf{b}$  satisfying  $dq(\mathbf{b}) = 1$  has Fisher information

$$\mathbf{F}_{\downarrow}(\mathbf{b}, \mathbf{b}) = F_{bb} = A^2 \,, \tag{3.39}$$

making this Fisher matrix the embodiment of one-from-many estimation: no matter what are the coördinates other than  $\phi = q$ , the Fisher information is the same (all **b** have the same Fisher length).

The Fisher ellipsoid degenerates to a pair of level surfaces of q having opposite values of q. Equivalent to Eq. (3.39) is that for any vector  $\mathbf{v}$  that lies in the level surface q = 0, i.e.,  $dq(\mathbf{v}) = 0$ ,

$$F_{\downarrow}(\boldsymbol{v}, \boldsymbol{v}) = 0 = F_{\downarrow}(\boldsymbol{v}, \boldsymbol{b})$$
 (3.40)

Quantum procedures that yield these Fisher matrices come up in Sec. VA.

# IV. QUANTUM ESTIMATION

# A. Quantum Cramér-Rao bound

Return now to the quantum setting, abandoned at the end of Sec. II. Quantum mechanics generates the classical conditional probability  $p(x|\tilde{\theta})$  from an initial state  $\rho$ , which is processed through a quantum process  $\mathcal{E}_{\tilde{\theta}}$  to give a state,

$$\rho_{\tilde{\theta}} = \mathcal{E}_{\tilde{\theta}}(\rho) \,, \tag{4.1}$$

and a measurement described by a POVM  $\{E_x\}$ , whose outcome x is the data collected by the measurement:

$$p(x|\tilde{\theta}) = \operatorname{tr}(E_x \rho_{\tilde{\theta}}). \tag{4.2}$$

Appreciate that in the quantum setting, the Fisher-information matrix and its Fisher ellipsoid are functions of the initial state  $\rho$  and the quantum measurement used to extract data from the system.

The foundation of quantum single-parameter estimation is the quantum Fisher information, defined at the fiducial state  $\rho = \rho_0$  by

$$Q_{bb} = \max_{\text{measurements}|\rho_0} F_{bb} = \text{tr}(\rho_0 L_b^2), \qquad (4.3)$$

$$\boldsymbol{b}\rho_{\tilde{\theta}}\big|_{\tilde{\theta}=0} = \frac{\partial \rho_{\tilde{\theta}}}{\partial \phi}\bigg|_{\tilde{\theta}=0} = \frac{1}{2}(\rho_0 L_b + L_b \rho_0). \tag{4.4}$$

The Hermitian operator  $L_b$  sports the title of symmetric logarithmic derivative (SLD); notice that  $tr(\rho_0 L_b) = 0$ . Foundation the quantum Fisher information is because according to Eq (4.3), it is the same as the classical Fisher information for the best quantum measurement; hence, find the bound

$$F_{bb} \le Q_{bb} \,. \tag{4.5}$$

The result is a chain of bounds on estimator variance:

$$\Delta \hat{\phi}^2 \ge \frac{1}{F_{bb}} \ge \frac{1}{Q_{bb}}.\tag{4.6}$$

The chain can be saturated: the first inequality, asymptotically in many trials, by using, for example, maximum-likelihood estimation; the second by choice of optimal quantum measurement.

Consider now unitary operations, as in Eq. (2.1), where  $\rho_{\tilde{\theta}} = \mathcal{U}_{\tilde{\theta}}(\rho)$ . The Hamiltonian (2.4), written in terms of the new parameters  $\tilde{\phi}$  and associated generators, becomes

$$H(\tilde{\theta}) = \phi^j Y_j = \phi Y + \sum_{i=2}^N \phi^j Y_j = H(\tilde{\phi}). \tag{4.7}$$

Here  $Y_j = \partial H/\partial \phi^j = (\partial \theta^k/\partial \phi^j)X_k = b^k{}_jX_k$ . Generating changes in  $\phi = q$  is the operator

$$Y = Y_1 = b^k X_k = \mathbf{b} H(\tilde{\theta}) = \frac{\partial H(\tilde{\theta})}{\partial \phi}. \tag{4.8}$$

Cumbersome indeed is the implicit expression (4.4) for determining the SLD  $L_b$ , but an appealingly simple, explicit form is available for a unitary process,  $\rho_{\tilde{\theta}} = \mathcal{U}_{\tilde{\theta}}(\rho) = e^{-iH(\tilde{\theta})}\rho e^{iH(\tilde{\theta})}$ , applied to a pure fiducial state  $\rho = |\psi\rangle\langle\psi|$ . For a unitary process, it is always true that

$$\frac{\partial \rho_{\tilde{\theta}}}{\partial \phi} \bigg|_{\tilde{\theta} = 0} = -i[Y, \rho] = -i[\Delta Y, \rho]; \tag{4.9}$$

introduction of the operator deviation  $\Delta Y = Y - \langle Y \rangle = Y - \operatorname{tr}(\rho Y)$  makes life easier shortly. Realize now that for a pure fiducial state, since  $\rho_{\tilde{\theta}} = \rho_{\tilde{\theta}}^2$ , have we

$$\frac{\partial \rho_{\tilde{\theta}}}{\partial \phi} = \rho_{\tilde{\theta}} \frac{\partial \rho_{\tilde{\theta}}}{\partial \phi} + \frac{\partial \rho_{\tilde{\theta}}}{\partial \phi} \rho_{\tilde{\theta}} \tag{4.10}$$

and the conclusion,

$$L_b = 2 \left. \frac{\partial \rho_{\tilde{\theta}}}{\partial \phi} \right|_{\tilde{\theta} = 0} = -2i[\Delta Y, \rho]. \tag{4.11}$$

Simple now is the quantum Fisher information (4.3):

$$Q_{bb} = -4\operatorname{tr}((\Delta Y \rho - \rho \Delta Y)^{2} \rho) = 4\langle (\Delta Y)^{2} \rangle. \tag{4.12}$$

The variance of the generator Y is calculated in the fiducial (pure) system state  $\rho$ .

Confronting us again, now in the quantum setting, are the requirements for defining a single-parameter estimation problem. The generator  $Y = \boldsymbol{b}H(\tilde{\theta})$ , whose variance is the quantum Fisher information, is determined by the vector  $\boldsymbol{b}$  that defines the single-parameter problem. The Hamiltonian (4.7) emphasizes that the parameters that accompany  $\phi$  must be held fixed to get a clean estimate of  $\phi = q$ .

One more inequality,

$$Q_{bb} = 4\langle (\Delta Y)^2 \rangle \le ||Y||_s^2 = ||\boldsymbol{b}H(\tilde{\theta})||_s^2. \tag{4.13}$$

completes the quantum discussion, by introducing the operator seminorm  $||Y||_s$ ,<sup>11</sup> the difference between the largest and smallest eigenvalues of Y. Add yet one more bound to the chain of single-parameter estimator bounds (4.5),

$$\Delta \hat{\phi}^2 \ge \frac{1}{F_{bb}} \ge \frac{1}{Q_{bb}} \ge \frac{1}{\|\mathbf{b}H(\tilde{\theta})\|_{o}^2}.$$
 (4.14)

Saturated is the last inequality by choosing an optimal fiducial state, an equal superposition of the eigenstates of Y with largest and smallest eigenvalues. Equally deserving the appellation of quantum Cramér-Rao bound (QCRB) are the last two inequalities; distinguish them by letting the first be the QCRB and the second, the focus of our attention because of its optimal fiducial-state, the QCRB-O.

Quantum Fisher information also comes in a multiparameter version, in which it is a positive matrix that defines a quadratic form on the space of parameters. With no need for this quantum Fisher matrix, tarry not to introduce it. The quantum Fisher matrix enjoys only a vestigial presence in our treatment: labeling the single-parameter quantum Fisher information as the bb component of a quantum Fisher matrix.

Focused though we are on unitary processes, realize that arbitrary processes can be included by employing the same reasoning to develop a process-dependent norm optimized over general (including mixed) initial states  $\rho$ . Not required for unitary processes, yet natural in developing the process norm is to generalize the optimization of states and measurements to be over an extended Hilbert space that includes ancillas in addition to the original system, even though the process itself acts only on the original system. The parametrized family of final states becomes  $\rho_{\tilde{\theta}} = (\mathcal{I} \otimes \mathcal{E}_{\tilde{\theta}})(\rho)$ . Thus define the process norm,

$$\|\boldsymbol{b}\|_{\mathcal{E}_{\tilde{\theta}}}^2 = \max_{\rho} Q_{bb} = \max_{\rho} \operatorname{tr}(\rho L_b^2) = \max_{\rho} \max_{\text{measurements}|\rho} F_{bb}, \qquad (4.15)$$

and generalize the chain (4.14) of inequalities to

$$\Delta \hat{\phi}^2 \ge \frac{1}{F_{bb}} \ge \frac{1}{Q_{bb}} \ge \frac{1}{\|\boldsymbol{b}\|_{\mathcal{E}_{\tilde{\theta}}}^2}.$$
 (4.16)

More detail for this norm—indeed, that it is a norm—comes in App. B.

Easy it is to imagine that ancillas permit joint measurements that can extract more information about the parameters, thus increasing the quantum Fisher information  $Q_{bb}$ . Indeed, the implicit definition (4.4) of the SLD indicates that  $L_b$  generally changes when one allows joint system-ancilla states  $\rho$ . Nonetheless, simple it is to argue that for a unitary process  $\mathcal{U}_{\tilde{\theta}}$ , as in Eq. (2.1), the process norm is

$$\|\boldsymbol{b}\|_{\mathcal{E}_{\tilde{\theta}}} = \|\boldsymbol{b}H(\tilde{\theta})\|_{s}, \qquad (4.17)$$

even after including ancillas. Suppose the maximum (4.15) for a unitary process occurs on a mixed state  $\rho$ . Purify  $\rho$  into further ancillas, and find that the maximum occurs on a pure state. Given that, run through the argument leading from Eq. (4.7) to Eq. (4.13), and conclude with the result (4.17) for the unitary process norm.

At first blush, nothing is gained for unitary processes by including ancillas in the definition of the process norm. On second look, however, there is a there there. Any extension to ancillas introduces degeneracies in the largest and smallest eigenvalues of the generator  $I \otimes \boldsymbol{b}H(\tilde{\theta})$ . Degeneracies give more possibilities for the optimal fiducial state, an equal superposition of states with largest and smallest eigenvalues; each such superposition has its own associated optimal measurement. These possibilities can be put to use in probabilistic protocols, which flip a coin to choose among different possibilities. Classical the coin can be, or quantum by encoding the coin into an entangled state.

In contrast to the universal expression for the process norm (4.17) for unitary processes, difficult it can be to evaluate the process norm for arbitrary processes. <sup>19–24</sup> Examples and explicit constructions in the remainder of this paper specialize to unitary processes, but the derived bounds and their achievability are applicable to arbitrary processes.

Now to one from many. Estimation of q, as explained in Sec. III C, is not the same as the single-parameter problem of estimating  $\phi = q$ . A fixed Fisher information, we saw in Sec. III D, allows identification of a special single-parameter problem that gives the appropriate one-from-many classical bound. Discovering an analogous single-parameter problem in the quantum setting, where the process norm replaces the fixed Fisher information, is the subject of the next subsection.

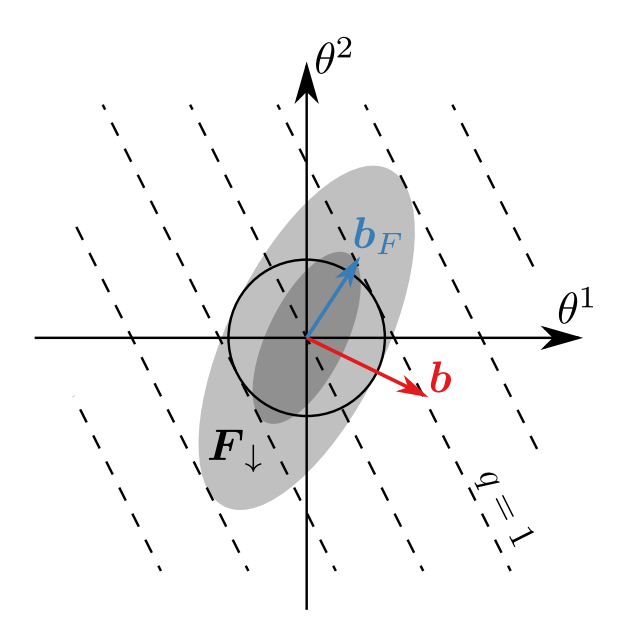


FIG. 5. For typical choices of  $\boldsymbol{b}$ , saturating the QCRB-O leaves the one-from-many (Cauchy-Schwarz) inequality unsaturated:  $\boldsymbol{F}_{\downarrow}(\boldsymbol{b}_F, \boldsymbol{b}_F) < F_{bb} = \|\boldsymbol{b}\|_{\mathcal{E}_{\bar{\theta}}}^2$ . The black circle represents the QCRB-O, demarking the minimum width of a Fisher ellipsoid in all directions. The light-gray ellipse represents the CCRB on the multiparameter estimator covariance given by a particular preparation/measurement protocol. Maximized by this protocol is the single-parameter Fisher information  $F_{bb}$ , thus making  $F_{bb} = Q_{bb} = \|\boldsymbol{b}\|_{\mathcal{E}_{\bar{\theta}}}^2$ , since the covariance ellipse touches the quantum Cramér-Rao circle along the direction  $\boldsymbol{b}$ . But the shortest vector, according to  $\boldsymbol{F}_{\downarrow}$ , that extends one unit in q, is  $\boldsymbol{b}_F$ , not  $\boldsymbol{b}$ . Failure to saturate the one-from-many inequality is the result:  $\boldsymbol{F}(\boldsymbol{b}_F, \boldsymbol{b}_F) < F_{bb}$ .

#### B. Scalar estimation

Fuse the classical one-from-many bound (3.35) with the single-parameter quantum bound (4.16) to obtain the ultimate chain:

$$\Delta \hat{q}^2 = \mathbf{C}^{\uparrow}(dq, dq) \ge \mathbf{F}^{\uparrow}(dq, dq) = \frac{1}{\mathbf{F}_{\downarrow}(\mathbf{b}_F, \mathbf{b}_F)} \ge \frac{1}{F_{bb}} \ge \frac{1}{Q_{bb}} \ge \frac{1}{\|\mathbf{b}\|_{\mathcal{E}_{\tilde{a}}}^2}.$$
 (4.18)

Short-circuit from now on the first link in this chain, our interest being to work in terms of classical Fisher ellipsoids, and the link through the quantum Fisher information  $Q_{bb}$ , our quantum interest being to go directly to the ultimate bound of optimized initial state, in which case  $Q_{bb} = \|\boldsymbol{b}\|_{\mathcal{E}_{\tilde{\theta}}}^2$ . Upside-down turn the chain (4.18), to work for convenience with Fisher informations:

$$\mathbf{F}_{\downarrow}(\mathbf{b}_F, \mathbf{b}_F) \le F_{bb} \le \|\mathbf{b}\|_{\mathcal{E}_{\tilde{a}}}^2$$
 (4.19)

The first inequality is one-from-many (or Cauchy-Schwarz); the second, the QCRB-O. Pose now a new question: for what  $\boldsymbol{b}$  are these two inequalities saturated? More precisely, is there a single-parameter problem defined by  $\boldsymbol{b}$ ,  $dq(\boldsymbol{b})=1$ , with an optimal estimation protocol (saturating the QCRB-O inequality) where errors in estimates of the other parameters that

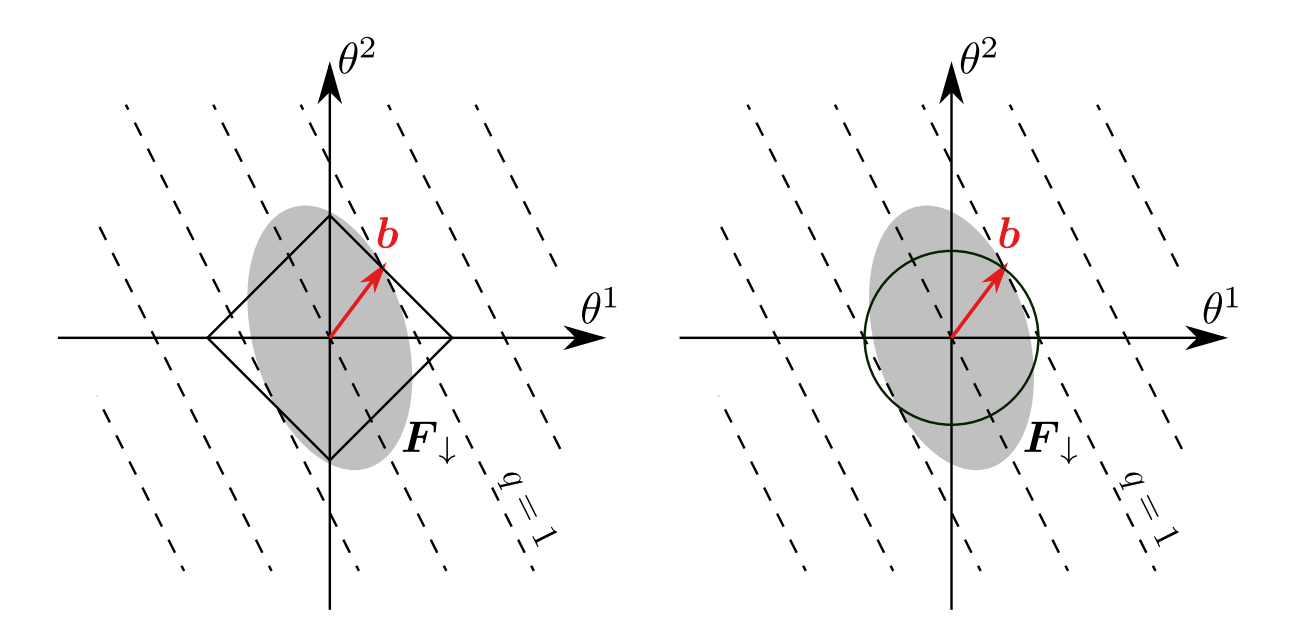


FIG. 6. If the surface of constant QCRB-O passing through the tip of b also passes through the unit surface of q, impossible it is for  $b = b_F$ , since this would imply the Fisher ellipsoid enters the interior of the surface of constant QCRB-O norm. Illustrated here is how this works for a nonmetric (square) QCRB-O surface (left) and a metric (circular) QCRB-O surface (right).

are irrelevant to q are uncorrelated with errors in the single parameter associated with b (saturating the one-from-many inequality)?

Available already is the condition for saturating the one-from-many inequality: The tip of  $\boldsymbol{b}$  must be at a point of tangency between the unit surface of q and a Fisher covariance ellipsoid of some measurement  $\boldsymbol{F}_{\downarrow}$ .

Developing a similiar geometric picture for the second inequality is the task now. To the fore comes the norm defined by the QCRB-O,  $\|\boldsymbol{b}\|_{\mathcal{E}_{\tilde{\theta}}}^2$ , and as the geometric object of interest, the "circle" of vectors of constant QCRB-O norm. Before optimization over initial states, the quantum Fisher-information matrix is a quadratic form, whose "circles" of constant norm are ellipsoids. As  $\boldsymbol{b}$  changes direction, however, the optimal initial state changes. The reason for this change is clear in the unitary case, where changing the generator  $\boldsymbol{b}H(\tilde{\theta})$  changes the eigenstates with extremal eigenvalues from which the optimal state is built. The result is to give the QCRB-O norm more diverse, nonmetric unit-circle shapes, even shapes with corners. Draw surfaces of constant QCRB-O norm, which are free of the dependence on initial state that plagues surfaces of constant QCRB, always remembering that to saturate the QCRB-O as a single-parameter estimation problem for a particular  $\boldsymbol{b}$  requires using an optimal initial state for  $\boldsymbol{b}$  and making the corresponding optimal measurement.

Useful it is to note that the QCRB-O unit "ball," *i.e.*, the circle of unit process norm and the interior of the circle, as the intersection of the Fisher ellipsoids for all measurements and all fiducial states, is an (absolutely) convex set. More technical discussion of the process norm and its unit ball is given in App. B.

A single-parameter problem must simultaneously saturate the one-from-many inequality and the QCRB-O in order to qualify as no-control estimation. As illustrated in Fig. 5, saturating the QCRB-O does not guarantee that the one-from-many inequality is saturated,

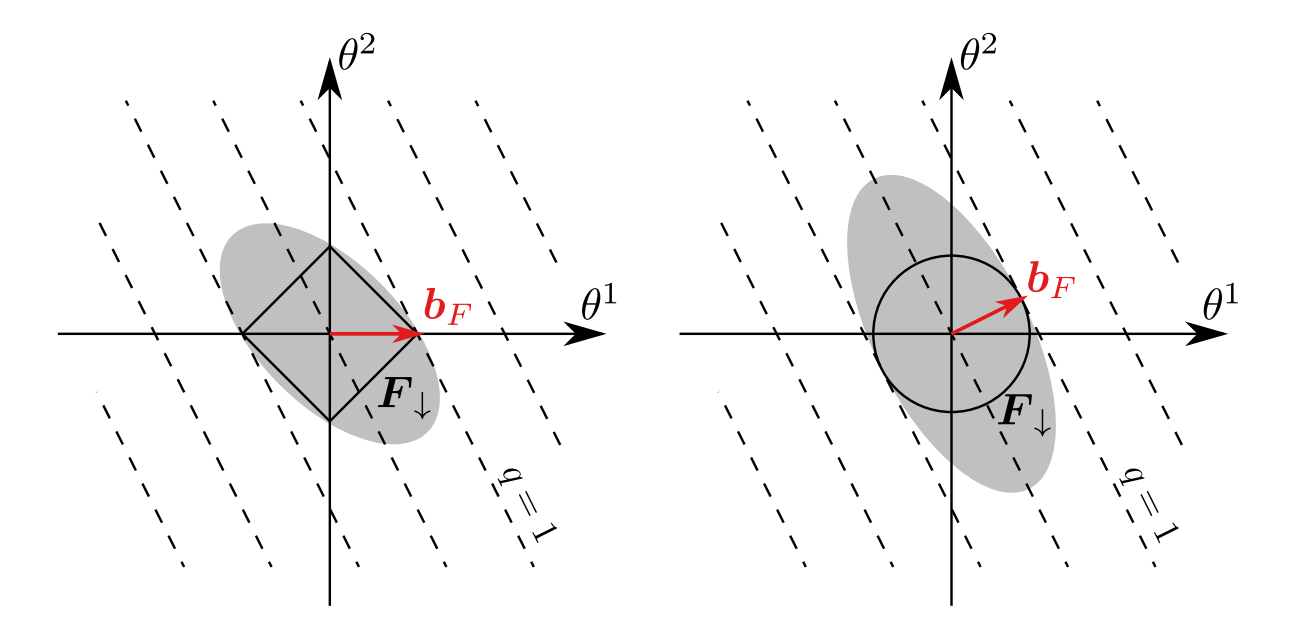


FIG. 7. If the surface of constant QCRB-O passing through the tip of  $\boldsymbol{b}$  does not pass through the unit surface of q, one can draw an ellipsoid tangent to the level surfaces of q at the tip of  $\boldsymbol{b}$  that remains outside the QCRB-O surface. This ellipsoid corresponds to a Fisher information that makes  $\boldsymbol{b} = \boldsymbol{b}_F$ . Illustrated here is how this works for a nonmetric (square) QCRB-O surface (left) and a metric (circular) QCRB-O surface (right). The vector  $\boldsymbol{b}$  is the shortest vector satisfying  $dq(\boldsymbol{b}) = 1$  according to the QCRB-O norm.

because an initial state and measurement procedure that saturate the QCRB-O for some b generally has a vector  $b_F$ , the shortest vector according to the classical Fisher metric for this state and measurement, that is different from b. Likewise, saturating the one-from-many inequality does not guarantee saturation of the QCRB-O.

To find conditions for the two vectors to coincide, draw a vector  $\mathbf{b}$  satisfying  $dq(\mathbf{b}) = 1$  and then the surface of constant QCRB-O norm that passes through the tip of  $\mathbf{b}$ . The optimal initial state and optimal measurement that attain the QCRB-O for  $\mathbf{b}$  have a Fisher ellipsoid,  $F_{vv} = F_{bb} = \|\mathbf{b}\|_{\mathcal{E}_{\bar{\theta}}}^2$ , that passes through the tip of  $\mathbf{b}$ ; the QCRB (4.19) implies that this Fisher ellipsoid cannot enter the interior of the surface of constant QCRB-O norm. But if we are to have  $\mathbf{b} = \mathbf{b}_F$  for this measurement, then the Fisher ellipsoid is tangent to the unit surface of q at  $\mathbf{b} = \mathbf{b}_F$ .

Close in on the quarry: conclude that the surface of constant QCRB-O norm cannot pass through the unit surface of q as in Fig. 6; it must kiss that surface as in Fig. 7. If the surfaces of constant QCRB-O norm are smooth, this kissing is tangency; if not, only kissing. Now the kill: conclude further, using the argument used for Fisher ellipsoids, that  $\boldsymbol{b}$  is the shortest vector  $\boldsymbol{b}_{\min}$ , according to the QCRB-O norm, whose tip lies on the unit surface of q,

$$\boldsymbol{b}_{\min} = \arg\min_{\boldsymbol{b}} \left\{ \|\boldsymbol{b}\|_{\mathcal{E}_{\tilde{\boldsymbol{\theta}}}}^{2} \mid dq(\boldsymbol{b}) = 1 \right\}. \tag{4.20}$$

One question yet remains: is it always possible to saturate the one-from-many (Cauchy-Schwarz) inequality by discovering a state preparation and measurement protocol such that  $b_F = b_{\min}$ ? One cannot fail if the Cramér–Rao unit circle is smooth at  $b_{\min}$ . As illustrated

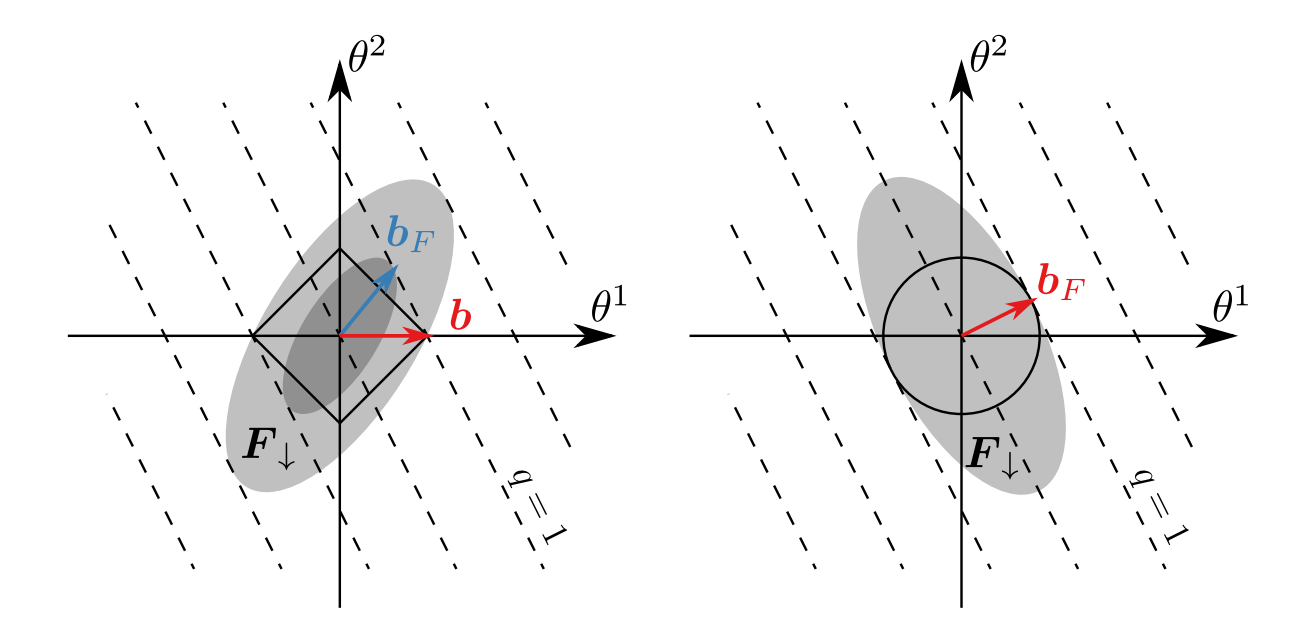


FIG. 8. For smooth QCRB-O unit circles (illustrated at right), saturating covariance ellipses have a unique tangent to the unit circle that must match the level surfaces of dq. At corners (illustrated at left), there are many tangents that a saturating covariance ellipse might make, so it is not guaranteed to be tangent to the level surfaces of dq.

in Fig. 8, all measurements saturating QCRB-O for a smooth unit circle have a Fisher ellipsoid that is tangent to the unit level surface of q, thus also saturating one-from-many. Care is required if the unit circle is pointed at  $b_{\min}$ : QCRB-O-saturating protocols generally have measurements with Fisher ellipsoids that pass through the q=1 surface, thus failing to saturate one-from-many, but measurements that do the job can be constructed. In particular, probabilistic measurement procedures transform extremal QCRB-O-saturating protocols into protocols that also saturate the one-from-many inequality, as illustrated in Fig. 9 and demonstrated in App. D.

Contemplate the happy situation: the Fisher ellipsoid for the measurement-state combination and the surface of constant QCRB-O norm both kiss the unit surface of q at  $\boldsymbol{b}_{\min}$ , with the Fisher ellipsoid lying (inclusively) between the QCRB-O surface and the unit surface of q. Understood is that tangency and kissing include the case where surfaces coincide; then "shortest" means "no shorter," and a kiss generalizes to a more generous smooth across a portion of a planar surface.

A Fisher ellipsoid has a tangent plane that kisses the unit surfaces of q at  $\boldsymbol{b}_{\min}$  if and only if (i)  $\boldsymbol{b}_{\min} = \boldsymbol{b}_F$ , *i.e.*, all  $\boldsymbol{v}_{\perp}$  that don't change q, are orthogonal to  $\boldsymbol{b}_{\min}$  according to the Fisher metric,

$$F_{\downarrow}(\boldsymbol{b}_{\min}, \boldsymbol{v}_{\perp}) = 0 = \|\boldsymbol{b}_{\min}\|_{\mathcal{E}_{\tilde{a}}}^{2} dq(\boldsymbol{v}_{\perp}),$$
 (4.21)

and (ii) the Fisher information therefore saturates both inequalities in (4.19),

$$F_{bb} = \mathbf{F}_{\downarrow}(\mathbf{b}_{\min}, \mathbf{b}_{\min}) = \|\mathbf{b}_{\min}\|_{\mathcal{E}_{\tilde{\theta}}}^{2} = \|\mathbf{b}_{\min}\|_{\mathcal{E}_{\tilde{\theta}}}^{2} dq(\mathbf{b}_{\min}). \tag{4.22}$$

Combining Eqs. (4.21) and (4.22) gives a single unified kissing condition,

$$F_{\downarrow}(\boldsymbol{b}_{\min}, \boldsymbol{v}) = \|\boldsymbol{b}_{\min}\|_{\mathcal{E}_{\tilde{\boldsymbol{\theta}}}}^2 dq(\boldsymbol{v}) \text{ for all } \boldsymbol{v},$$
 (4.23)

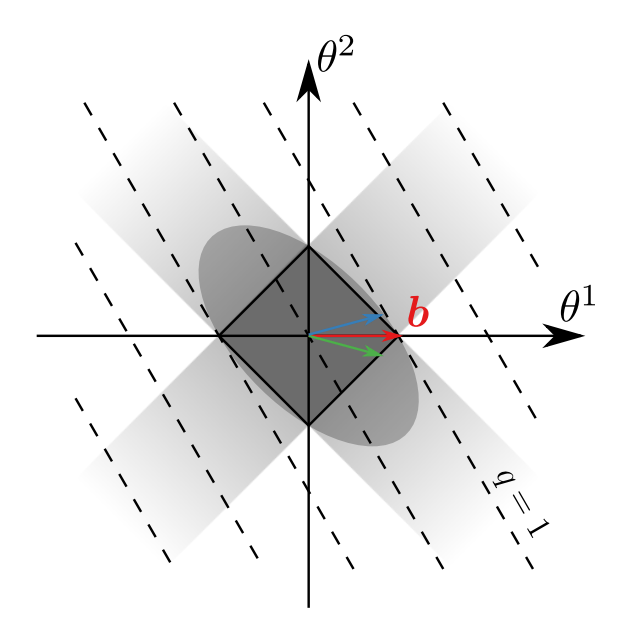


FIG. 9. When the shortest b according to the QCRB-O norm lies on a corner of the unit circle, measurements that saturate the quantum QCRB-O bound for nearby parameters (the blue and green arrows) also saturate the QCRB-O bound for b. These covariance ellipses have infinite extent in parameters tangent to the unit circle at these nearby points, so the tangents they make to the corner are the most extreme possible. Flipping a coin to choose between protocols that saturate the quantum Cramér-Rao bounds for these nearby parameters leads to covariance ellipses that still saturate the quantum Cramér-Rao bound for b while making a tangent to the corner that interpolates between the extreme tangents. Choose therefore the probabilities to create a tangent that matches the level surfaces of dq, simultaneously saturating the one-from-many inequality and the QCRB-O bound.

which is equivalent to

$$F_{jk}b_{\min}^{j} = \|\boldsymbol{b}_{\min}\|_{\mathcal{E}_{\tilde{\boldsymbol{\theta}}}}^{2}q_{k} \iff b_{\min}^{j} = \|\boldsymbol{b}_{\min}\|_{\mathcal{E}_{\tilde{\boldsymbol{\theta}}}}^{2}q^{j}. \tag{4.24}$$

Explore this answer through examples in Sec. V, but before doing so, clarify in the next subsection that there are other ways to perform what might be called no-control estimation and how these are related to the results in this paper.

# C. Intervention techniques

Easy it is to imagine protocols that rescale the parameters in the unitary operator  $e^{-iH(\bar{\theta})}=e^{-i\theta^j X_j}$  by changing the constants that couple a generator to the system or, equivalently, by adjusting separately the evolution times for those generators. Spin echo can accomplish this effect without directly adjusting coupling constants or evolution times. Such rescaling effectively changes the Hamiltonian, yet might be regarded as a no-control protocol, since rather than directly controlling an underlying parameter in the Hamiltonian, the protocol controls quantities, associated with a generator, that are generally available to an agent in charge of a metrological experiment. Appreciating this argument, nonetheless

we stick with the approach outlined up till now: the family of processes  $\mathcal{E}_{\tilde{\theta}}$  is part of the statement of the problem—completely specified by the Hamiltonian  $H(\tilde{\theta}) = \theta^j X_j$  for unitary processes; separate scaling of the parameters via intervention techniques leads to a problem that, though readily analyzed by the techniques developed in this paper, is nonetheless a different problem. Tying the notion of a parameter to the process family and sticking with that notion fixes the method by which the parameters are impressed on the system, enabling us to extract a magic number from the process family, the ultimate quantum limit given by the square of the process norm  $\|\boldsymbol{b}_{\min}\|_{\mathcal{E}_{\tilde{\theta}}}^2$ , which for unitary processes becomes the squared seminorm of the generator,  $\|\boldsymbol{b}_{\min}H(\tilde{\theta})\|_s^2$ .

## V. EXAMPLES: PUTTING THE FORMALISM TO WORK

# A. Commuting generators

## 1. Setup

Consider now the scenario introduced by Eldredge *et al.*<sup>12</sup>: the parameters  $\theta^j$  are rotation angles about the Bloch z axis for different qubits; hence, the generators are Pauli z operators  $\sigma_i^z$  for the various qubits, giving Hamiltonian

$$H(\tilde{\theta}) = \frac{1}{2}\theta^j \sigma_j^z \,. \tag{5.1}$$

For convenience and without any loss of generality, discard qubits that do not contribute to q, *i.e.*, for which  $q_j = 0$ ; order the remaining qubits so that the absolute value of  $q_j$  descends through the list of qubits; and scale q such that  $q_1 = 1$ , thus giving  $1 = q_1 \ge |q_2| \ge \cdots \ge |q_N| > 0$ .

For an arbitrary vector  $\boldsymbol{b} = b^j \partial_j$ , the single-parameter generator and QCRB-O norm are

$$Y = \mathbf{b}H(\tilde{\theta}) = \frac{1}{2}b^j\sigma_j^z, \qquad (5.2)$$

$$\|\boldsymbol{b}H(\tilde{\theta})\|_{s} = \frac{1}{2}\|b^{j}\sigma_{j}^{z}\|_{s} = \sum_{j=1}^{N}|b^{j}| = \|\boldsymbol{b}\|_{1}.$$
 (5.3)

Here  $\|\boldsymbol{b}\|_1$  is the 1-norm of the vector  $\boldsymbol{b}$ .

The geometric object of interest is the QCRB-O unit surface,  $\|\boldsymbol{b}\|_1 = 1$ . This, the unit cross-polytope in N dimensions, is the dual of the unit hypercube. In three dimensions, the cross-polytope is the octahedron. A hyperface of the cross-polytope lies in the unit plane defined by a linear function  $z = z_j \theta^j$ , with  $z_j = \pm 1$ . Indeed, a hyperface is the intersection of the cross-polytope with the unit plane of z,

$$dz(\mathbf{b}) = \mathbf{b}z = z_j b^j = 1. (5.4)$$

Here  $dz = z_j d\theta^j$  is the 1-form corresponding to z. Thus define a hyperface of the cross-polytope by

$$\left\{ \boldsymbol{b} \mid z_j b^j = 1 \quad \text{and} \quad \sum_{j=1}^N |b^j| = 1 \right\}. \tag{5.5}$$

Stress that the sign of  $b^j$  is  $z_j$ , implying that  $b^j = z_j |b^j|$  (no sum). Convenient and productive it is to let a string  $\mathbf{z} = z_1 \dots z_N$  list the coefficients  $z_j$  and so specify a hyperface.

Construct first in Sec. V A 2 measurements optimal for a q that coincides with a hyperface z, *i.e.*, dq = dz; then use these measurements in Sec. V A 3 as ingredients in the recipe for measurements optimal at the QCRB-O corners that arise for general q.

## 2. Hyperface measurements

When the unit surface of q coincides with a hyperface z there are many choices for  $\boldsymbol{b}_{\min}$  (any vector in the hyperface z will do). Aesthetic sensibilities direct us to  $\boldsymbol{b}_{\min}$  with components  $b^j = 1/z_j N$ . The generator associated with this choice,

$$Y = \mathbf{b}_{\min} H(\tilde{\theta}) = \frac{1}{2} \frac{1}{z_i N} \sigma_j^z, \qquad (5.6)$$

has extremal eigenvalues  $\pm \frac{1}{2}$  associated with the eigenvectors

$$|\pm \mathbf{z}\rangle = \bigotimes_{j=1}^{N} |\pm z_j\rangle. \tag{5.7}$$

Here  $|z_j\rangle$  is the eigenstate of  $\sigma_j^z$  with eigenvalue  $z_j$ , i.e.,  $\sigma_j^z|z_j\rangle = z_j|z_j\rangle$ , and  $-\mathbf{z}$  is the string with the sign of all the entries reversed, i.e.,  $-\mathbf{z} = -z_1 \dots -z_N$ ;  $\mathbf{z}$  and  $-\mathbf{z}$  specify opposite faces of the cross-polytope. The normalized states  $|\mathbf{z}\rangle$  are orthogonal:

$$\langle \mathbf{z} | \mathbf{z}' \rangle = \prod_{j=1}^{N} \langle z_j | z_j' \rangle = \delta_{\mathbf{z}\mathbf{z}'}.$$
 (5.8)

Define cat-superposition states,

$$|\psi_{\mathbf{z}}^{(\pm)}\rangle = \frac{1}{\sqrt{2}}(|\mathbf{z}\rangle \pm |-\mathbf{z}\rangle)$$
 (cat state), (5.9)

$$|\psi_{\mathbf{z}}^{(\pm i)}\rangle = \frac{1}{\sqrt{2}}(|\mathbf{z}\rangle \pm i|-\mathbf{z}\rangle) \quad (i\text{cat state}).$$
 (5.10)

Any of these choices work as the initial state for an optimal estimation strategy. Choosing  $|\psi_{\mathbf{z}}^{(+)}\rangle$  and imposing the parameters via  $H(\tilde{\theta})$  yields the final state

$$e^{-iH(\tilde{\theta})}|\psi_{\mathbf{z}}^{(+)}\rangle = \frac{1}{\sqrt{2}} \left( e^{-iz_j\theta^j/2} |\mathbf{z}\rangle + e^{iz_j\theta^j/2} |-\mathbf{z}\rangle \right). \tag{5.11}$$

Measure now in an orthonormal basis containing  $|\psi_{\mathbf{z}}^{(\pm i)}\rangle$  (the basis elements in the subspace orthogonal to the span of  $|\mathbf{z}\rangle$  and  $|-\mathbf{z}\rangle$  are superfluous, since the final state has no support on that subspace). Appendix C shows how to think of the needed measurement as a parity measurement and thus how to implement it locally.

The probabilities for the results corresponding to states  $|\psi_{\mathbf{z}}^{(\pm i)}\rangle$  are

$$p(\pm|\tilde{\theta}) = \left| \langle \psi_{\mathbf{z}}^{(\pm i)} | e^{-iH(\tilde{\theta})} | \psi_{\mathbf{z}}^{(+)} \rangle \right|^2 = \frac{1}{4} \left| e^{-iz_j \theta^j/2} \mp i e^{iz_j \theta^j/2} \right|^2 = \frac{1}{2} \left( 1 \pm \sin z_j \theta^j \right), \tag{5.12}$$

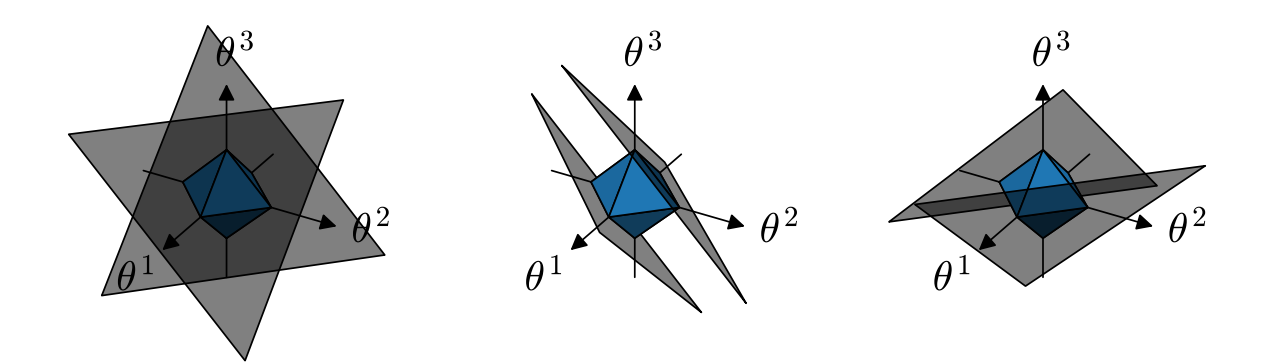


FIG. 10. A sampling of Fisher "ellipsoids" for hyperface measurements in the case N=3, where the QCRB-O unit surface, the N=3 cross-polytrope, is the (blue) octahedron. The hyperfaces are depicted by pairs of shaded triangles bounding the covariance regions. The chosen samples correspond to the Fisher informations  $\mathbf{F}_{\downarrow}^{(k)}$  used to saturate QCRB-O when all  $q_j > 0$ . The corresponding  $\mathbf{z}$  strings are, from left to right, 111, 1–1–1, and 11–1.

leading to Fisher-information matrix

$$F_{jk} = \sum_{\pm} \frac{1}{p(\pm|\tilde{\theta}=0)} \left. \frac{\partial p(\pm|\tilde{\theta})}{\partial \theta^j} \right|_{\tilde{\theta}=0} \left. \frac{\partial p(\pm|\tilde{\theta})}{\partial \theta^k} \right|_{\tilde{\theta}=0} = z_j z_k; \tag{5.13}$$

i.e.,  $\mathbf{F}_{\downarrow} = dz \otimes dz$  is the degenerate Fisher matrix for no-control estimation of q=z discussed at the end of Sec. III D.

Verify that the tangency condition (4.24) is met for  $q_j = z_j$ , noting that  $\|\boldsymbol{b}_{\min}H(\tilde{\theta})\|_s = \|\boldsymbol{b}_{\min}\|_1 = 1$ :

$$F_{jk}b_{\min}^{j} = \sum_{j=1}^{N} z_{j}z_{k} \frac{1}{z_{j}N} = z_{k} = \|\boldsymbol{b}_{\min}H(\tilde{\theta})\|_{s}^{2}q_{k}.$$
 (5.14)

Figure 10 illustrates the Fisher "ellipsoids" for several of these optimal measurements in the case N=3.

# 3. Getting away with kissing at corners

Arbitrary q, put in the canonical form described in Sec. VA1, now comes to the fore. Broken is the symmetry of q = z; the unit cross-polytope is only guaranteed to touch the unit surface of q at one point,

$$\boldsymbol{b}_{\min} = \partial_1. \tag{5.15}$$

This vector lives at the corner of the unit circle just like the vector in Fig. 9. Implement the probabilistic corner strategy discussed at the end of Sec. IV B: construct a Fisher ellipsoid

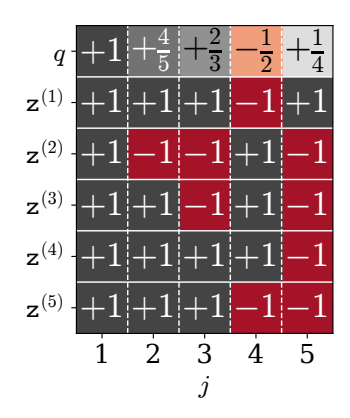


FIG. 11. Illustration of the special strings  $\mathbf{z}^{(k)}$  for  $q = \theta^1 + \frac{4}{5}\theta^2 + \frac{2}{3}\theta^3 - \frac{1}{2}\theta^2 + \frac{1}{4}\theta^5$ . The parameters  $\theta^j$  have been ordered such that  $|q_j| \ge |q_k|$  for  $k \ge j$ .

whose tangent surface matches the level surfaces of q at  $\boldsymbol{b}_{\min}$  (and hence saturates the one-from-many inequality) by using a convex combination of Fisher informations saturating the QCRB-O on the hyperfaces adjacent to that corner.

Define the strings  $\mathbf{z}^{(k)}$  corresponding to the adjacent hyperfaces,

$$z_j^{(1)} = \operatorname{sgn} q_j = \begin{cases} 1 & q_j > 0 \\ -1 & q_j < 0 \end{cases}, \tag{5.16}$$

$$z_j^{(k>1)} = \begin{cases} z_j^{(1)} & \text{if } j < k, \\ -z_j^{(1)} & \text{if } j \ge k \end{cases}, \tag{5.17}$$

$$dz^{(k)} = z_1^{(1)} d\theta^1 + \dots + z_{k-1}^{(1)} d\theta^{k-1} - z_k^{(1)} d\theta^k - \dots - z_N^{(1)} d\theta^N.$$
 (5.18)

Figure 11 depicts these strings for a particular q when N=5. Appreciate now two important properties of these strings: first,  $\{dz^{(k)}\}$  is a basis of forms; second, the coefficients of dq in this basis are positive and normalized to unity—they make up a probability distribution. Specifically,

$$dq = \sum_{k=1}^{N} p_k dz^{(k)}, \qquad (5.19)$$

with

$$p_1 = \frac{1}{2} (1 + |q_N|), \qquad (5.20)$$

$$p_{k>1} = \frac{1}{2} (|q_{k-1}| - |q_k|). \tag{5.21}$$

The Fisher informations for the hyperface measurements are  $\mathbf{F}_{\downarrow}^{(k)} = dz^{(k)} \otimes dz^{(k)}$ . Performing the  $\mathbf{F}^{(k)}$  measurement with probability  $p_k$  yields the new Fisher information,  $\mathbf{F}_{\downarrow} =$ 

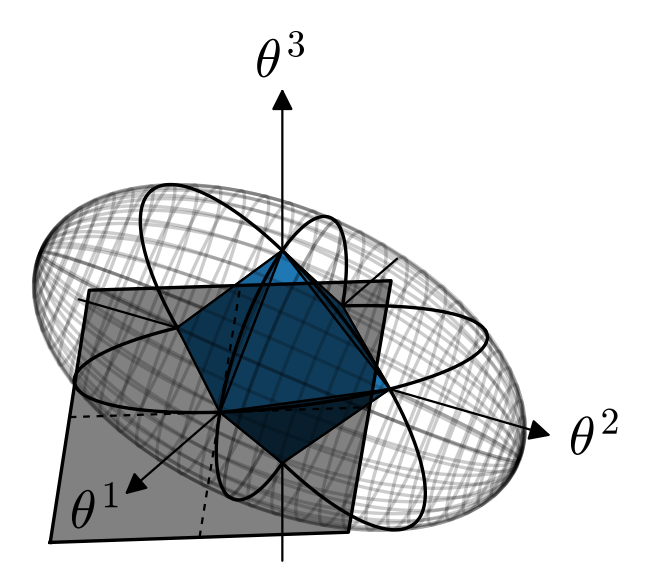


FIG. 12. The Fisher information (illustrated as a mesh ellipsoid) whose tangent plane at  $\boldsymbol{b}_{\min} = \partial_1$  (illustrated as the shaded plane) is a level surface of  $q = \theta^1 + \frac{2}{3}\theta^2 + \frac{1}{3}\theta^3$ . This ellipsoid contacts the QCRB-O unit circle,  $\|\boldsymbol{b}\|_{\mathcal{U}_{\tilde{\theta}}} = \|\boldsymbol{b}H(\tilde{\theta})\|_s = 1$ , illustrated as the blue octahedron, at all vertices.

 $\sum_{k} p_{k} \mathbf{F}_{\downarrow}^{(k)}$ . Appendix D explains why such a protocol is allowed and why the Fisher information takes this form. Verify now that the kissing condition (4.23) is satisfied:

$$\boldsymbol{F}_{\downarrow}(\boldsymbol{b}_{\min}, \boldsymbol{v}) = \sum_{k=1}^{N} p_k dz^{(k)}(\boldsymbol{v}) = \|\boldsymbol{b}H(\tilde{\theta})\|_s^2 dq(\boldsymbol{v}).$$
 (5.22)

Fig. 12 illustrates a Fisher information constructed according to this recipe.

Similar in spirit is this construction to that in Sec. IV B 1 of Eldredge *et al.*<sup>12</sup> Appendix E explores a zoo of variations on these sorts of measurements.

### B. Noncommuting generators

Turn now to noncommuting generators. As a simple example, consider the Hamiltonian for a single qubit:

$$H(\theta^1, \theta^2, \theta^3) = \frac{1}{2} \left( \theta^1 \sigma^x + \theta^2 \sigma^y + \theta^3 \sigma^z \right) = \frac{1}{2} \boldsymbol{\theta} \cdot \boldsymbol{\sigma}.$$
 (5.23)

Here introduce, by necessity, a bastard inner product that recognizes the natural Euclidean geometry of the Bloch sphere. The Euclidean geometry runs rough-shod over the distinction between upper and lower indices; using dot notation for this inner product sidesteps ugly sums over indices that are both upper or both lower.

The generator for a vector  $\mathbf{b} = b^j \partial_j$ ,

$$Y = \boldsymbol{b}H(\theta^1, \theta^2, \theta^3) = \frac{1}{2} \left( b^1 \sigma^x + b^2 \sigma^y + b^3 \sigma^z \right) = \frac{1}{2} \boldsymbol{b} \cdot \boldsymbol{\sigma},$$
 (5.24)

gives QCRB-O seminorm

$$\|\mathbf{b}H(\theta^1, \theta^2, \theta^3)\|_s = \sqrt{(b^1)^2 + (b^2)^2 + (b^3)^2} = \sqrt{\mathbf{b} \cdot \mathbf{b}} = \|\mathbf{b}\|_2,$$
 (5.25)

with  $\|\boldsymbol{b}\|_2$  being the Euclidean length of  $\boldsymbol{b}$ . The QCRB-O unit circle is the Euclidean unit sphere.

Now estimate linear combination  $q = q_j \theta^j$ . Tangent to the QCRB-O sphere the unit plane of q must be; scaling q appropriately, this means that  $q_j = b^j$ , which also yields the desired  $dq(\mathbf{b}) = q_j b^j = \mathbf{b} \cdot \mathbf{b} = 1$ . The rest is standard qubitology. Use as fiducial state an optimal state for generator (5.24), say,  $|\psi\rangle = (|\mathbf{b}\rangle + |-\mathbf{b}\rangle)/\sqrt{2}$ . After imposition of the parameters by Hamiltonian (5.23), measure in the basis  $|\psi_{\mathbf{b}}^{(\pm i)}\rangle = (|\mathbf{b}\rangle \pm i|-\mathbf{b}\rangle)/\sqrt{2}$ . The outcome probabilities,

$$\left| \left\langle \psi_{\mathbf{b}}^{(\pm i)} \middle| e^{-iH(\boldsymbol{\theta})} \middle| \psi \right\rangle \right|^2 = \frac{1}{2} [1 \pm \sin(\mathbf{b} \cdot \boldsymbol{\theta})] = \frac{1}{2} [1 \pm \sin(q_j \theta^j)], \qquad (5.26)$$

depend only on the component of  $\boldsymbol{\theta}$  along  $\boldsymbol{b}$ . Realize with satisfaction that this component—the summation convention rightly restored!—is the property q itself, which gives the rotation angle about  $\boldsymbol{b}$  that is being measured. The result? A no-control Fisher-information matrix  $F_{jk} = q_j q_k$ , whose Fisher ellipsoid consists of the two planes tangent to the unit sphere at the tips of  $\boldsymbol{b}$  and  $-\boldsymbol{b}$ .

Observe more interesting behavior by varying the degree to which the generators fail to commute, as in the two-qubit Hamiltonian

$$H(\theta^1, \theta^2) = \frac{1}{2} \left[ \theta^1 \left( \sigma_1^z + \sqrt{2\epsilon} \, \sigma_2^x \right) + \theta^2 \sigma_2^z \right]. \tag{5.27}$$

The generator for vector  $\boldsymbol{b} = b^j \partial_j$ ,  $Y = \boldsymbol{b} H(\tilde{\theta}) = \frac{1}{2} \left[ b^1 \left( \sigma_1^z + \sqrt{2\epsilon} \, \sigma_2^x \right) + b^2 \sigma_2^z \right]$ , has seminorm

$$\|\mathbf{b}H(\theta^1, \theta^2)\|_s = |b^1| + \sqrt{(b^2)^2 + 2\epsilon(b^1)^2}$$
. (5.28)

Figure 13 illustrates how the QCRB-O unit circle changes as the process generators become increasingly noncommuting. The smooth curves of the unit circle are serviced by optimal measurements like those just encountered for the three Pauli operators; the corners present opportunities for measurements like those encountered for commuting generators in Sec. V A.

To assess those opportunities, notice that vectors on the upper  $(b^2 \ge 0)$  part of the QCRB-O unit circle take the form

$$\mathbf{b} = b^1 \partial_1 + \sqrt{1 - 2|b^1| + (1 - 2\epsilon)(b^1)^2} \,\partial_2. \tag{5.29}$$

The generators associated with the vectors are

$$Y = \frac{1}{2} \left[ b^{1} \sigma_{1}^{z} + (1 - |b_{1}|) \, \hat{\boldsymbol{n}} \cdot \boldsymbol{\sigma}_{2} \right],$$

$$\hat{\boldsymbol{n}} = \frac{\sqrt{1 - 2|b^{1}| + (1 - 2\epsilon)(b^{1})^{2}} \, \hat{\boldsymbol{z}} + b^{1} \sqrt{2\epsilon} \, \hat{\boldsymbol{x}}}{1 - |b^{1}|}.$$
(5.30)

The extremal eigenvalues of Y,  $\pm \frac{1}{2}$ , correspond to eigenvectors  $|\pm \operatorname{sgn}(b^1)\hat{z}\rangle \otimes |\pm \hat{n}\rangle$ . The corresponding optimal measurement is a hyperface measurement, like those in Sec. VA2, except that on the second qubit the z direction is replaced by  $\hat{n}$ .

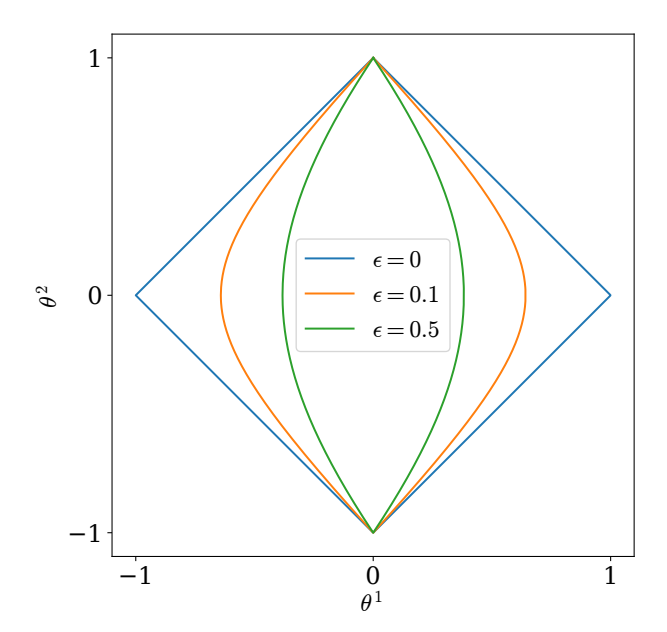


FIG. 13. Process norms for several generator pairs ranging from commuting ( $\epsilon = 0$ ) to increasing degrees of noncommutivity. The cross polytope indicative of commutivity becomes rounded at two of its corners as  $\epsilon$  grows.

Focus now on the upper cusp of the unit circle of  $\|\boldsymbol{b}\|_{\mathcal{U}_{\bar{\theta}}}$ . Consider a scalar  $q=q_1\theta^1+q_2\theta^2$ , where  $q_1< q_2=1$ . The unit surface of q touches the QCRB-O unit circle at the upper cusp,  $\boldsymbol{b}_{\min}=\partial_2$ . Near the cusp, regardless of the value of  $\epsilon$ , the QCRB-O unit circle looks like the square that applies for  $\epsilon=0$ ; for the vectors of Eq. (5.29), as  $|b^1|\to 0$ ,  $\hat{\boldsymbol{n}}\to\hat{\boldsymbol{z}}$ , and the measurements are the two hyperface measurements, for  $b^1>0$  and  $b^1<0$ , considered in Sec. V A 2. Matching the tangent made by q is then carried out just as it was in Sec. V A 3.

# VI. CONCLUSION

Laid to rest is the question of ultimate, achievable precision in the estimation of scalar properties of arbitrary quantum channels. Tempted to stray from the straight, but narrow path by superficial similarities to single-parameter estimation, we stayed the course by keeping eyes fixed on the distinction between the differential forms defining our problem and the tangent vectors defining single-parameter problems. Yet unwise it would have been to disregard completely the voice of those who have trod the single-parameter road, for from their stores of knowledge came forth the process norm on the tangent space. By examining the relation between this process norm and the differential form of the scalar property of interest, all becomes clear, and maximally precise scalar estimation strategies emerge, beautiful to behold, constructed from the optimal single-parameter strategies known from old.

In light of these investigations of parameter estimation, as was said over two thousand years ago, so still it must be said, "Let no one ignorant of geometry enter here."

# Appendix A: Estimator bias

Worthwhile it is to consider sensing small deviations away from a true value that is itself close to the fiducial operating point ( $\hat{\theta} = 0$ ). Typical this situation is, and it is the situation considered in this paper.

In this situation, calculate the Fisher information at the fiducial point, instead of at the (unknown) true point, *i.e.*,

$$F_{jk} = \int dx \, p(x|\tilde{\theta} = 0) \, \frac{\partial \ln p(x|\tilde{\theta})}{\partial \theta^j} \Bigg|_{\tilde{\theta} = 0} \, \frac{\partial \ln p(x|\tilde{\theta})}{\partial \theta^k} \Bigg|_{\tilde{\theta} = 0}; \tag{A1}$$

likewise, the Jacobian of the mean estimates should be calculated at the fiducial point,

$$J^{j}{}_{k} = \left. \frac{\partial \langle \hat{\theta}^{j} \rangle_{\tilde{\theta}}}{\partial \theta^{k}} \right|_{\tilde{\theta}=0} . \tag{A2}$$

Not knowing the true parameter values, we are commanded to do things this way for the tensor formalism to make sense.

Approximate can we also the means of the estimators by expanding about the fiducial point:

$$\langle \hat{\theta}^j \rangle_{\tilde{\theta}} = \langle \hat{\theta}^j \rangle_{\tilde{\theta}=0} + \left. \frac{\partial \langle \hat{\theta}^j \rangle_{\tilde{\theta}}}{\partial \theta_k} \right|_{\tilde{\theta}=0} \theta^k = \langle \hat{\theta}^j \rangle_{\tilde{\theta}=0} + J^j{}_k \theta^k \,. \tag{A3}$$

If  $\hat{\theta}^{j}(x)$  is a biased estimator, an associated estimator  $\hat{\theta}^{j}(x)$  can be defined by

$$\hat{\bar{\theta}}^{j}(x) = (J^{-1})^{j}_{k} \left[ \hat{\theta}^{k}(x) - \langle \hat{\theta}^{k} \rangle_{\tilde{\theta}=0} \right], \tag{A4}$$

and the new estimator is unbiased.

$$\langle \hat{\theta}^j \rangle_{\tilde{\theta}} = \theta^j \,. \tag{A5}$$

The offset removes bias at the fiducial point; the inverse of the Jacobian removes scaling and mixing that introduce bias away from the fiducial point. Able to do this, we can and should always do it and thus use the multiparameter CCRB for unbiased estimators; it then is a matter of indifference whether we use the error-correlation matrix or the covariance matrix to state the CCRB.

#### Appendix B: Process norm

Defined in Eq. (4.15) is the process norm. Appreciate first that this is a norm. From Eq. (4.15), discern that the associated unit ball is the intersection of the unit covariance ellipsoids of all possible Fisher informations. The length that our potential norm assigns to any vector is the smallest positive scaling of the unit ball that contains the vector. A norm must assign a finite, nonnegative value to every vector; satisfy the triangle inequality  $(\|\boldsymbol{v} + \boldsymbol{w}\| \leq \|\boldsymbol{b}\| + \|\boldsymbol{w}\|)$ ; be absolutely scalable  $(\|\lambda\boldsymbol{v}\| = |\lambda|\|\boldsymbol{v}\|)$ ; and be nondegenerate  $(\|\boldsymbol{v}\| = 0 \Rightarrow \boldsymbol{v} = \boldsymbol{0})$ . The first three properties correspond to the unit ball being an

absolutely convex absorbing set, and the nondegeneracy corresponds to the unit ball being bounded.

A norm we have because the unit ball is absolutely convex, being an intersection of ellipsoids, which are absolutely convex; absorbing, not assigning infinite length to any vector **b**, since that would correspond to infinite estimation precision; and bounded, not assigning zero length to any vector, since we assume that deviations in all parameters are detectable (*i.e.*, there are no physically meaningless parameters).

# Appendix C: Parity measurements and icat states

The icat states  $|\psi_{\mathbf{z}}^{(\pm i)}\rangle$  of Eq. (5.10) are eigenstates of  $(\sigma^y)^{\otimes N}$  when N is odd and  $(\sigma^y)^{\otimes N-1}\otimes\sigma^x$  when N is even. Understand why by recalling  $\sigma^y|z_j\rangle=|z_j|-z_j\rangle$  and  $\sigma^x|z_j\rangle=|-z_j\rangle$ . For N odd,

$$(\sigma^{y})^{\otimes N} |\psi_{\mathbf{z}}^{(\pm i)}\rangle = \frac{i^{N}}{\sqrt{2}} (z_{1} \cdots z_{N}) (|-\mathbf{z}\rangle \pm (-1)^{N} i |\mathbf{z}\rangle)$$

$$= \mp (-1)^{(N+1)/2} (z_{1} \cdots z_{N}) |\psi_{\mathbf{z}}^{(\pm i)}\rangle,$$
(C1)

and for N even,

$$(\sigma^{y})^{\otimes N-1} \otimes \sigma^{x} |\psi_{\mathbf{z}}^{(\pm i)}\rangle = \frac{i^{N-1}}{\sqrt{2}} (z_{1} \cdots z_{N-1}) (|-\mathbf{z}\rangle \pm (-1)^{N-1} i |\mathbf{z}\rangle)$$

$$= \mp (-1)^{N/2} (z_{1} \cdots z_{N-1}) |\psi_{\mathbf{z}}^{(\pm i)}\rangle.$$
(C2)

Measuring these generalized parity operators realizes an optimal measurement for the protocols in Sec. V A 2.

#### Appendix D: Probabilistic protocols

Probabilistic protocols we invoke in Sec. IV B to argue that measurements saturating the one-from-many inequality always exist for  $b_{\min}$ . Understand now the precise nature of these probabilistic protocols and the means by which they achieve our aim.

Given two different measurement protocols, each dictating the preparation of a particular initial state and the measurement of a particular POVM, one can combine the two by deciding to choose randomly which protocol to follow before making use of the channel of interest. The bounds in this paper are derived allowing for the possibility of entangled ancillas. Since random choice between different state preparation and measurement can be effected by a deterministic protocol using entangled ancillas, a probabilistic protocol along these lines is allowed within the quantum framework of Sec. IV A. Entangled protocols find a place in the examples of App. E 2.

The *n*th deterministic protocol has fiducial state  $\rho_n$  and measures POVM  $\{E_{x_n}\}$ , labeled by outcomes  $x_n$ ; the outcomes have probability  $p(x_n|n,\tilde{\theta}) = \operatorname{tr}(\rho_{n,\tilde{\theta}}E_{x_n})$ , where  $\rho_{n,\tilde{\theta}} = \mathcal{E}_{\tilde{\theta}}(\rho_n)$  is the output of the quantum process. The probabilistic protocol has all the outcomes of all the deterministic protocols; the probability of outcome  $x_n$  is

$$p(x_n|\tilde{\theta}) = p(x_n|n,\tilde{\theta})p(n), \qquad (D1)$$

where p(n) is the probability to choose the *n*th deterministic protocol. Now easy it is to see that the Fisher information for the probabilistic protocol is the convex combination of the Fisher informations for the deterministic protocols:

$$F_{jk} = \sum_{n} \int dx_{n} \frac{1}{p(x_{n}|\tilde{\theta})} \partial_{j} p(x_{n}|\tilde{\theta}) \partial_{k} p(x_{n}|\tilde{\theta})$$

$$= \sum_{n} p(n) \int dx_{n} \frac{1}{p(x_{n}|n,\tilde{\theta})} \partial_{j} p(x_{n}|n,\tilde{\theta}) \partial_{k} p(x_{n}|n,\tilde{\theta})$$

$$= \sum_{n} p(n) F_{jk}(n) .$$
(D2)

Return now to the problem of constructing an optimal probabilistic protocol at a corner  $b_{\min}$  of the QCRB-O surface. Consider all the b near to  $b_{\min}$  that have the same QCRB-O norm. In a small enough neighborhood, this looks like the boundary of a convex cone, called the tangent cone. Identifying tangent planes to this cone with forms results in the construction of the dual cone. We show that all the tangent planes to the tip of the tangent cone—that is, all forms in the dual cone—can be expressed as convex combinations of tangent planes to smooth points on the tangent cone. Since there always exists a quantum protocol realizing at least one tangent plane to a point on the cone, and since smooth points only have one tangent plane, this implies that arbitrary tangent planes to the tip of the cone can be realized through probabilistic combinations of quantum protocols that are known to exist.

We first eliminate irrelevant parameters so the base of the restricted tangent cone is bounded. If the surface of constant QCRB-O norm is flat in certain directions at  $\boldsymbol{b}_{\min}$  (for example, if it is a sphere) the tangent cone extends infinitely in that direction. The level surfaces of dq coincide exactly with the tangent cone in those directions, as does the covariance of any QCRB-O-saturating measurement protocol, so we can safely ignore those directions and restrict to the remaining cone, whose base is a bounded convex set just like the unit ball of our norm. A smooth point on the boundary of this set corresponds to a ray of smooth points on the boundary of the tangent cone.

We now argue that the set of extremal tangent planes to this restricted tangent cone is equivalent to the set of tangent planes to its base. Extremal tangent planes are rotated out as far away as possible from being flat at the tip of the cone, so they are entirely determined by the lower-dimensional tangent plane they make with the base of the cone. Combine this with the observation that a lower-dimensional tangent plane to a smooth point on the base corresponds to a tangent plane to a smooth point on the cone, since the additional degree of freedom in the cone is a ray emanating from the tip, and therefore smooth.

We use this trick of reducing the dimension to bootstrap a higher-dimensional protocol from lower-dimensional protocols. Start by assuming we can make arbitrary tangent planes to any point on the boundary of this lower-dimensional convex set using a convex combination of tangent planes to smooth points in the neighborhood of that point. From this it would follow that we can make arbitrary extremal tangent planes to the point of interest in our higher-dimensional convex set using convex combinations of tangent planes to smooth points. Since the dual cone of tangent planes is convex, probabilistic protocols for making extremal tangent planes yield probabilistic protocols for making all tangent planes. For a two-dimensional cone it is easy to see how to make arbitrary tangent planes to its base using convex combinations of tangent planes to smooth points, since the base is a

one-dimensional object and both points on the boundary are smooth. Inductively, one can then build up convex combinations of smooth tangent planes to construct arbitrary tangent planes of higher-and-higher-dimensional convex sets, ultimately arriving at a probabilistic protocol that matches the level surface of dq at the point of interest.

Summarize: make arbitrary tangent planes to a point of interest on the unit ball by utilizing lower-dimensional protocols for making arbitrary tangent planes to points on the boundary of the base of the tangent cone of the point of interest.

# Appendix E: A zoo of measurements in the commuting case

Hyperface measurements are the focus of Sec. V A 2, because they are sufficient for constructing the optimal protocols needed in Sec. V A. Yet these are far from the only deterministic measurement protocols that saturate the QCRB-O. As additional examples, consider hyperedges of the cross-polytope, specified by a string  $\mathbf{w} = w_1 \dots w_N$ , much like the string for a hyperface, except that the characters can be 0 in addition to 1 and -1. The hyperedges so signified are

$$\left\{ \boldsymbol{b} \mid w_j b^j = 1 \quad \text{and} \quad \sum_{j=1}^N |b^j| = 1 \right\}. \tag{E1}$$

In three dimensions—the cross-polytope is an octahedron—the six vertices correspond to the six strings with two zeroes, the twelve edges to the twelve strings with one zero, and the eight faces to the eight strings with no zeroes. For example,  $\mathbf{w} = 0 - 10$  is the vertex on the negative y axis,  $\mathbf{w} = -101$  is the edge that connects the -x axis with the positive z axis, and  $\mathbf{w} = 1 - 11$  is the face in the octant defined by the +x, -y, and +z axes. Generally, there are 2N vertices corresponding to strings with N-1 zeroes;  $2^N$  faces corresponding to strings with no zeroes; and  $2^K N!/K!(N-K)!$  hyperedges of dimension K—these we call K-hyperedges—corresponding to strings with N-K zeroes.

Consider now achieving the QCRB-O in a no-control estimation of  $q = q_j \theta^j$  (recall that we assume that  $|q_j| \leq 1, j = 1, \ldots, n$ ) for a vector  $\boldsymbol{b}$  that lies on the unit surface of q and also lies in the interior of a K-hyperedge of the cross-polytope specified by string  $\boldsymbol{w}$ . The discussion at Eq. (E1) leads to

$$\mathbf{b} = \sum_{j=1}^{N} w_j |b^j| \partial_j, \qquad \|\mathbf{b}\|_1 = \sum_{j=1}^{N} |b^j| = 1.$$
 (E2)

According to the discussion in Sec. IV B, the cross-polytope must kiss the unit surface of q at  $\mathbf{b}$ . Hence, coincide with the K-hyperedge the unit surface of q must, meaning that  $q_j = w_j$  for  $w_j = \pm 1$ , with the other  $q_j$ s left arbitrary. Summarize: the linear combinations for which one-from-many and QCRB-O can be simultaneously saturated at  $\mathbf{b}$  of Eq. (E2)—notice that  $dq(\mathbf{b}) = 1$ —are

$$q = \sum_{\{j|w_j = \pm 1\}} w_j \theta^j + \sum_{\{j|w_j = 0\}} q_j \theta^j = w + \sum_{\{j|w_j = 0\}} q_j \theta^j, \quad |q_j| \le 1.$$
 (E3)

# 1. Measurements sensitive only to the parameters on a hyperedge

Specialize now to no-control measurements that are sensitive only to the parameters on a hyperedge, i.e., q = w. Construct the states necessary for hyperedge measurements by considering the zero-including strings w. Let  $\mathbf{w}^1$  be the string in which all the zeroes in w are replaced by +1:

$$|\mathbf{w}^{1}\rangle = \bigotimes_{\{j|w_{j}=\pm 1\}} |w_{j}\rangle \bigotimes_{\{j|w_{j}=0\}} |+1\rangle. \tag{E4}$$

Appreciate that in -w, all the zero entries remain zero, so those entries become +1 in  $(-w)^1$ , giving

$$|(-\mathbf{w})^{\mathbf{1}}\rangle = \bigotimes_{\{j|w_j = \pm 1\}} |-w_j\rangle \bigotimes_{\{j|w_j = 0\}} |+1\rangle. \tag{E5}$$

Note carefully that the strings w and -w specify opposite K-hyperedges of the cross-polytope, whereas  $w^1$  and  $(-w)^1$  specify hyperfaces that contain these opposite K-hyperedges, but also share hyperedges that are specified by the 1s held in common by  $w^1$  and  $(-w)^1$ .

Introduce the analog of the cat and icat states of Eqs. (5.9) and (5.10):

$$|\psi_{\mathbf{w}^{1}}^{(\pm)}\rangle = \frac{1}{\sqrt{2}} (|\mathbf{w}^{1}\rangle \pm |(-\mathbf{w})^{1}\rangle),$$
 (E6)

$$|\psi_{\mathbf{w}^{1}}^{(\pm i)}\rangle = \frac{1}{\sqrt{2}} (|\mathbf{w}^{1}\rangle \pm i|(-\mathbf{w})^{1}\rangle). \tag{E7}$$

Understand that in these states, unlike the cat and icat states, the (irrelevant) qubits that have  $w_j = 0$  are in a product of +1 eigenstates of  $\sigma^z$ . Any of these states is an optimal states for **b** of Eq. (E2); other optimal state can be constructed using any state for the irrelevant qubits, but the product of +1 eigenstates is convenient.

Use these new states as ingredients in the standard recipe. Let the qubits begin in the state  $|\psi_{\mathbf{v}^{1}}^{(+)}\rangle$ . Imposition of the parameters leads to the state

$$e^{-iH(\tilde{\theta})}|\psi_{\mathbf{w}^{1}}^{(+)}\rangle = \frac{1}{\sqrt{2}} \left( e^{-iw_{j}\theta^{j}/2} |\mathbf{w}^{1}\rangle + e^{iw_{j}\theta^{j}/2} |(-\mathbf{w})^{1}\rangle \right) \exp\left( -\frac{i}{2} \sum_{\{j|w_{j}=0\}} \theta^{j} \right).$$
 (E8)

The irrelevant qubits, in state  $|+1\rangle$  in both parts of the superposition, contribute the final phase factor, which has no effect on measurement probabilities. Make a measurement in the orthonormal basis consisting of  $|\psi_{\mathtt{w}^1}^{(\pm i)}\rangle$  and the product states  $|\mathtt{z}\rangle$ , with  $\mathtt{z} \neq \mathtt{w}^1, (-\mathtt{w})^1$ . Results  $\mathtt{z}$  have zero probability, and the probabilities for the results corresponding to  $|\psi_{\mathtt{w}^1}^{(\pm i)}\rangle$  are

$$p(\pm|\tilde{\theta}) = \left| \langle \psi_{\mathbf{w}^{1}}^{(\pm i)} | e^{-iH(\tilde{\theta})} | \psi_{\mathbf{w}^{1}}^{(+)} \rangle \right|^{2} = \frac{1}{4} \left| e^{-iw_{j}\theta^{j}/2} \mp ie^{iw_{j}\theta^{j}/2} \right|^{2} = \frac{1}{2} \left( 1 \pm \sin w_{j}\theta^{j} \right), \tag{E9}$$

leading to Fisher-information matrix

$$F_{jk} = \sum_{\pm} \frac{1}{p(\pm|\tilde{\theta} = 0)} \left. \frac{\partial p(\pm|\tilde{\theta})}{\partial \theta^j} \right|_{\tilde{\theta} = 0} \left. \frac{\partial p(\pm|\tilde{\theta})}{\partial \theta^k} \right|_{\tilde{\theta} = 0} = w_j w_k$$
 (E10)

or, equivalently,

$$\mathbf{F}_{\downarrow} = dw \otimes dw = dq \otimes dq \,. \tag{E11}$$

This estimation scenario gathers information only about the property  $q = w = w_j \theta^j$ . For any vector  $\boldsymbol{v}$ , we have

$$F_{vv} = F_{jk}v^{j}v^{k} = (w_{j}v^{j})^{2} = [dw(\mathbf{v})]^{2}.$$
 (E12)

which has the value 1 for any vector on the unit surface of w (the vector need not be confined to the portion of that surface that is the hyperedge  $\mathbf{w}$  of the polytope). For a vector  $\mathbf{b}$  on the hyperedge specified by  $\mathbf{w}$ , as in Eq. (E2),

$$1 = dw(\mathbf{b}) = w_j b^j = \sum_j |b^j| = ||\mathbf{b}||_1 = ||\mathbf{b}H(\tilde{\theta})||_s,$$
 (E13)

so the measurement satisfies the unified kissing condition (4.23),

$$\mathbf{F}_{\downarrow}(\mathbf{b}, \mathbf{v}) = \|\mathbf{b}H(\tilde{\theta})\|_{s}^{2} dq(\mathbf{v}) \text{ for all } \mathbf{v},$$
 (E14)

and is an optimal no-control measurement of the parameter q=w, achieving both the one-from-many bound and the QCRB-O.

#### 2. A zoo of measurements

Return now to a property q of the general form (E3), and visit a zoo of varied optimal measurements that can be used for estimating q.

Specifying the fiducial state requires an ancillary qubit, which can be thought of as the zeroth qubit—let it appear on the far left of tensor products—and which does not participate in the parameter-dependent interaction. Necessary will it be to make one of the primary qubits special, as the primary qubit that is entangled with the ancillary qubit, and that special qubit might as well be the first.

Choose as fiducial state

$$|\psi\rangle = \sum_{\mathbf{z}} |z_1\rangle \otimes c_{\mathbf{z}} |\psi_{\mathbf{z}}^{(+)}\rangle = \sum_{\mathbf{z}} |z_1\rangle \otimes c_{\mathbf{z}} \frac{1}{\sqrt{2}} (|\mathbf{z}\rangle + |-\mathbf{z}\rangle);$$
 (E15)

Assume the amplitudes factor as

$$c_{\mathbf{z}} = c_{1,z_1} c_{z_2,...z_N};$$
 (E16)

squared, they are a probability distribution  $p_{\mathbf{z}} = |c_{\mathbf{z}}|^2 = p_{1,z_1} p_{z_2...z_N}$ . Unpack the notation to reveal what  $|\psi\rangle$  is:

$$|\psi\rangle = \sum_{z_1} c_{1,z_1} |z_1\rangle \otimes \sum_{z_2,\dots,z_N} c_{z_2\dots z_N} \frac{1}{\sqrt{2}} (|z_1, z_2, \dots, z_N\rangle + |-z_1, -z_2, \dots, -z_N\rangle).$$
 (E17)

This fiducial state could be created in the following way: start the primary qubits in the  $z_1 = +1$  state on the right of Eq. (E17), start the ancilla in the state  $\sum_{z_1} c_{1,z_1} |z_1\rangle$ , and run a controlled-NOT from the ancilla to the first primary qubit.

If only one  $c_{1,z_1}=1$  is nonzero, the ancillary qubit is not entangled with the primary qubits, and the state of the primary qubits is a superposition of cat states, each corresponding to opposite faces of the cross-polytope. If all the  $c_z=1/\sqrt{2^N}$  are equal, the ancillary qubit is not entangled with the primary qubits, and  $|\psi\rangle$  reduces to

$$|\psi\rangle = \frac{1}{\sqrt{2}} (|+1\rangle + |-1\rangle) \otimes \frac{1}{\sqrt{2^N}} \sum_{\mathbf{z}} |\mathbf{z}\rangle.$$
 (E18)

The sum over equal linear combination of all the basis states of the primary qubits is a product of +1  $\sigma^x$  eigenstates, so the entire state is a product of +1  $\sigma^x$  eigenstates for the ancillary qubit and the primary qubits.

Imposition of the parameters leads to

$$|\psi_{\tilde{\theta}}\rangle = e^{-iH(\tilde{\theta})}|\psi\rangle$$

$$= \sum_{\mathbf{z}} |z_{1}\rangle \otimes \frac{1}{\sqrt{2}} c_{\mathbf{z}} \left(e^{-iz_{j}\theta^{j}/2}|\mathbf{z}\rangle + e^{iz_{j}\theta^{j}/2}|-\mathbf{z}\rangle\right)$$

$$= \frac{1}{2} \sum_{\mathbf{z}} |z_{1}\rangle \otimes c_{\mathbf{z}} \left(\left(e^{-iz_{j}\theta^{j}/2} - ie^{iz_{j}\theta^{j}/2}\right)|\psi_{\mathbf{z}}^{(+i)}\rangle + \left(e^{-iz_{j}\theta^{j}/2} + ie^{iz_{j}\theta^{j}/2}\right)|\psi_{\mathbf{z}}^{(-i)}\rangle\right).$$
(E19)

Measure in the orthonormal basis consisting of states  $|z_1\rangle \otimes |\psi_{\mathbf{z}}^{(\pm i)}\rangle$ . The outcome probabilities,

$$p(\pm \mathbf{z}|\tilde{\theta}) = \left| \left( \langle z_1 | \otimes \langle \psi_{\mathbf{z}}^{(\pm i)} | \right) | \psi_{\tilde{\theta}} \rangle \right|^2 = \frac{1}{4} p_{\mathbf{z}} \left| e^{-iz_j \theta^j / 2} \mp i e^{iz_j \theta^j / 2} \right|^2 = \frac{1}{2} p_{\mathbf{z}} \left( 1 \pm \sin z_j \theta^j \right), \quad (E20)$$

give rise to Fisher-information matrix

$$F_{jk} = \sum_{\pm \mathbf{z}} \frac{1}{p(\pm \mathbf{z}|\tilde{\theta} = 0)} \left. \frac{\partial p(\pm \mathbf{z}|\tilde{\theta})}{\partial \theta^j} \right|_{\tilde{\theta} = 0} \left. \frac{\partial p(\pm \mathbf{z}|\tilde{\theta})}{\partial \theta^k} \right|_{\tilde{\theta} = 0} = \sum_{\mathbf{z}} p_{\mathbf{z}} z_j z_k = \overline{z_j z_k}, \tag{E21}$$

where a bar denotes an average over  $p_z$ . This Fisher information is a convex combination of the Fisher informations of the form (E10) for the case where the two hyperedges are opposite faces of the cross-polytope. Because  $z_i^2 = 1$ , the Fisher matrix (E21) has 1s on the diagonal.

The same result emerges if the pure fiducial state (E15) is replaced by the mixed state

$$\rho = \sum_{\mathbf{z}} p_{\mathbf{z}} |z_1\rangle \langle z_1| \otimes |\psi_{\mathbf{z}}^{(+)}\rangle \langle \psi_{\mathbf{z}}^{(+)}|.$$
 (E22)

This works because the measurement can be regarded as first determining whether  $z_1$  is  $\pm 1$ , then identifying a subspace spanned by a particular  $|\mathbf{z}\rangle$  and  $|-\mathbf{z}\rangle$  and then doing a measurement in the *i*cat basis  $|\psi_{\mathbf{z}}^{(\pm i)}\rangle$  within that subspace; coherence between these possibilities matters not.

Any vector  $\boldsymbol{v}$  has Fisher information

$$F_{vv} = F_{jk}v^jv^k = \sum_{\mathbf{z}} p_{\mathbf{z}}(z_jv^j)^2 = \sum_{\mathbf{z}} p_{\mathbf{z}}[dz(\mathbf{v})]^2.$$
 (E23)

If **b** points to a vertex on the j axis of the cross-polytope, i.e.,  $\mathbf{b} = \pm \partial_j$ , then  $dz(\mathbf{b}) = \pm z_j$  and  $F_{bb} = F_{jj} = 1$ . The Fisher ellipsoid circumscribes the vertices of the cross-polytope.

Specialize now to the case where the amplitudes and probabilities factor completely,

$$c_{\mathbf{z}} = \prod_{j=1}^{N} c_{j,z_j} = c_{1,z_1} \cdots c_{N,z_N}, \qquad p_{\mathbf{z}} = \prod_{j=1}^{N} p_{j,z_j} = p_{1,z_1} \cdots p_{N,z_N}.$$
 (E24)

The fiducial state (E17) becomes

$$|\psi\rangle = \frac{1}{\sqrt{2}} \left( \sum_{z_1} c_{1,z_1} |z_1\rangle \otimes |z_1\rangle \bigotimes_{j=2}^N \sum_{z_j} c_{j,z_j} |z_j\rangle + \sum_{z_1} c_{1,z_1} |z_1\rangle \otimes |-z_1\rangle \bigotimes_{j=2}^N \sum_{z_j} \sum_{z_j} c_{j,z_j} |-z_j\rangle \right). \tag{E25}$$

Only the marginals

$$\overline{z}_j = p_{j,+1} - p_{j,-1} = a_j \,,$$
 (E26)

which can take on values  $|a_i| \leq 1$ , matter now, with the Fisher matrix becoming

$$F_{jk} = \delta_{jk}(1 - a_j^2) + a_j a_k. (E27)$$

Worthwhile as an example is the case  $a_j = a, j = 1, ..., N$ . The Fisher ellipsoid has one minor axis,

$$\mathbf{v} = \frac{1}{\sqrt{N[1 + a^2(N-1)]}} \sum_{j} \partial_j, \qquad (E28)$$

which points directly into the all-positive  $2^N$ -ant; any vector  $\boldsymbol{u}$  that lies in the plane  $0 = \sum_j u^j$  and has  $\sum_j (u^j)^2 = (1-a^2)^{-1}$  is a major axis. For 0 < a < 1, the Fisher ellipsoid is prolate and circumscribes the cross-polytope. When a = 0, the Fisher ellipsoid becomes a sphere; when a = +1, it degenerates to the pair of planes  $\sum_j v^j = \pm 1$  and thus contains the paired all-positive and all-negative faces of the cross-polytope.

Return now to the Fisher information (E27). For specificity, consider the vertex  $\mathbf{w} = 10...0$  (the same construction works at any vertex). Vector  $\mathbf{b} = \partial_1$  points to this vertex. As promised by Eq. (E3), there should be an optimal no-control measurement of the parameter  $(\mathbf{w} = \theta^1)$ ,

$$q = \theta^1 + \sum_{j=2}^{N} q_j \theta^j, \quad |q_j| \le 1.$$
 (E29)

Required is that the Fisher ellipsoid be tangent to the level surface of q; thus demand that the gradient of the Fisher quadratic form,  $F_{jk}\theta^j\theta^k$ , be proportional to the gradient of q at  $\theta^j = \delta^j_1$ :

$$d\theta^{1} + \sum_{k=2}^{N} q_{k} d\theta^{k} = dq \propto d(F_{jk} \theta^{j} \theta^{k}) = 2F_{jk} \theta^{j} d\theta^{k} = 2F_{1k} d\theta^{k} = 2\left(d\theta^{1} + a_{1} \sum_{k=2}^{N} a_{k} d\theta^{k}\right).$$
(E30)

Choose

$$a_j = \begin{cases} 1, & j = 1, \\ q_j, & j = 2, \dots, N, \end{cases}$$
 (E31)

to make the proportionality, and—voilà!—find a no-control procedure for estimating q, achieving both the one-from-many and QCRB-O bounds.

Generalize this no-control measurement to a K-hyperedge. Let  $w = 1 \dots 10 \dots 0$ , where there are 1s in the first K positions and 0s in the remaining N - K slots (the same construction works for any K-hyperedge). A vector  $\boldsymbol{b}$  on the hyperedge has the form (E2):

$$\mathbf{b} = \sum_{k=1}^{K} b^k \partial_k, \qquad \sum_{k=1}^{K} b^k = 1, \quad b_k \ge 0.$$
 (E32)

To be estimated is a linear combination of the form (E3):

$$q = w + \sum_{k=K+1}^{N} q_k \theta^k = \sum_{k=1}^{K} \theta^k + \sum_{k=K+1}^{N} q_k \theta^k, \quad |q_k| \le 1.$$
 (E33)

Any point on the K-hyperedge satisfies  $\sum_{k=1}^{K} \theta^k = 1$ , with  $\theta^k \geq 0$ , for k = 1, ..., K, and  $\theta^k = 0$ , for k = K + 1, ..., N. The requirement that the Fisher ellipsoid be tangent to the level surface of q is again that at any point on the K-hyperedge, the gradient of the Fisher quadratic form  $F_{ik}\theta^j\theta^k$  be proportional to the gradient of q:

$$\sum_{k=1}^{K} d\theta^{k} + \sum_{k=K+1}^{N} q_{k} d\theta^{k} = dq$$

$$\propto 2F_{jk} \theta^{j} d\theta^{k} = 2\sum_{k=1}^{K} d\theta^{k} \left( \theta^{k} (1 - a_{k}^{2}) + a_{k} \sum_{j=1}^{K} a_{j} \theta^{j} \right) + 2\sum_{k=K+1}^{N} d\theta^{k} a_{k} \sum_{j=1}^{K} a_{j} \theta^{j}.$$
(E34)

Make the proportionality true by choosing

$$a_j = \begin{cases} 1, & j = 1, \dots, K, \\ q_j, & j = K + 1, \dots, N. \end{cases}$$
 (E35)

Thus generalized is Eq. (E31) to a no-control procedure for estimating property q of Eq. (E33), achieving both the one-from-many and QCRB-O bounds. Cylindrical is the Fisher ellipsoid for the measurement given by Eq. (E35): it contains the K-hyperedges  $\mathbf{w}$  and  $-\mathbf{w}$  and runs off to infinity along the planes defined by those hyperedges; the cross-section of the cylinder is an ellipsoid.

The choice (E35) is similar, yet different from the measurement formulated in App. E1. The difference? The measurement in App. E1 uses a fiducial state that makes the measurement insensitive to parameters  $\theta^k$  for k = K + 1, ..., N; the measurement here adjusts the fiducial state of the previously superfluous qubits to give just the right sensitivity to those

same parameters, thus delivering a procedure for no-control estimation of q in Eq. (E33), instead of estimation of w.

\* jarthurgross@gmail.com

- <sup>1</sup> R. A. Fisher, "On the mathematical foundations of theoretical statistics," Philosophical Transactions of the Royal Society of London A **222**, 309–368 (1922).
- <sup>2</sup> D. Dugué, "Application des propr'etés de la limite au sens du calcul des probabilités a l'étude des diverses questions d'estimation," Journal de l'Ecole Polytechnique **3**(4), 305–372 (1937).
- <sup>3</sup> C. R. Rao, "Information and the accuracy attainable in the estimation of statistical parameters," Bulletin of the Calcutta Mathematical Society **37**, 81–91 (1945); reprinted in *Breakthroughs in Statistics: Foundations and Basic Theory*, edited by S. Kotz and N. L. Johnson (Springer Science+Business Media, New York, 1992), pp. 235–247.
- <sup>4</sup> H. Cramér, Mathematical Methods of Statistics (Princeton University Press, 1946), p. 500.
- <sup>5</sup> H. L. van Trees, Detection, Estimation, and Modulation Theory. Part I. Detection, Estimation, and Linear Modulation Theory (Wiley-Interscience, New York, 2001), Chap. 2.
- <sup>6</sup> C. W. Helstrom, Quantum Detection and Estimation Theory (Academic Press, New York, 1976).
- <sup>7</sup> A. S. Holevo, Probabilistic and Statistical Aspects of Quantum Theory (North-Holland, Amsterdam, 1982).
- <sup>8</sup> W. K. Wootters, "Statistical distance and Hilbert space," Physical Review D 23, 357–362 (1981).
- <sup>9</sup> S. L. Braunstein and C. M. Caves, "Statistical distance and the geometry of quantum states," Physical Review Letters 72, 3439–3443 (1994).
- <sup>10</sup> S. L. Braunstein, C. M. Caves, and G. J. Milburn, "Generalized uncertainty relations: Theory, examples, and Lorentz invariance," Annals of Physics (N.Y.) **247**, 135–173 (1996).
- S. Boixo, S. T. Flammia, C. M. Caves, and J. Geremia, "Generalized limits for single-parameter quantum estimation," Physical Review Letters 98, 090401 (2007).
- <sup>12</sup> Z. Eldredge, M. Foss-Feig, J. A. Gross, S. L. Rolston, and A. V. Gorshkov, "Optimal and secure measurement protocols for quantum sensor networks," Physical Review A 97, 042337 (2018).
- <sup>13</sup> J. S. Sidhu and P. Kok, "A geometric perspective on quantum parameter estimation," arXiv:1907.06628 (2019).
- <sup>14</sup> M. G. A. Paris, "Quantum estimation for quantum technology," International Journal of Quantum Information **07**, 125–137 (2009).
- <sup>15</sup> T. J. Proctor, P. A. Knott, and J. A. Dunningham, "Multi-parameter estimation in networked quantum sensors," Physical Review Letters 120, 080501 (2018).
- <sup>16</sup> T. J. Proctor, P. A. Knott, and J. A. Dunningham, "Networked quantum sensing," arXiv:1702.04271 (2017).
- <sup>17</sup> K. S. Thorne, "John Archibald Wheeler: 1911–2008," arXiv:1901.06623, to be published in the Biographical Memoirs of the National Academy of Sciences and of the Royal Society.
- <sup>18</sup> For an imitation just of the idiosyncracy, see J. A. Wyler, "Rasputin, science, and the transmogrification of destiny," General Relativity and Gravitation 5, 175–182 (1974).
- A. Fujiwara and H. Imai, "A fibre bundle over manifolds of quantum channels and its application to quantum statistics," Journal of Physics A: Mathematical and Theoretical 41, 255304 (2008).

<sup>†</sup> ccaves@unm.edu

- R. Demkowicz-Dobrzański, J. Kołodyński, and M. Guţă, "The elusive Heisenberg limit in quantum-enhanced metrology," Nature Communications 3, 1063 (2012).
- J. Kołodyński and R. Demkowicz-Dobrzański, "Efficient tools for quantum metrology with uncorrelated noise," New Journal of Physics 15, 073043 (2013).
- <sup>22</sup> M. Tsang, "Quantum metrology with open dynamical systems," New Journal of Physics 15, 073005 (2013).
- S. Alipour, M. Mehboudi, and A. T. Rezakhani, "Quantum metrology in open systems: Dissipative Cramér-Rao bound," Physical Review Letters 112, 120405 (2014).
- <sup>24</sup> B. M. Escher, R. L. de Matos Filho, and L. Davidovich, "General framework for estimating the ultimate precision limit in noisy quantum-enhanced metrology," Nature Physics 7, 406–411 (2011).